AWARD NUMBER: W81XWH-16-1-0791

TITLE: Integration of the Residual Limb with Prostheses via Direct Skin-Bone-Peripheral Nerve Interface

PRINCIPAL INVESTIGATOR: Mark Pitkin

RECIPIENT: Poly-Orth International
Sharon MA 02067-1518

REPORT DATE: October 2018

TYPE OF REPORT: Annual

PREPARED FOR: U.S. Army Medical Research and Materiel Command
Fort Detrick, Maryland 21702-5012

DISTRIBUTION STATEMENT: Approved for Public Release; Distribution Unlimited

REPORT DOCUMENTATION PAGE

Form Approved
OMB No. 0704-0188

1. REPORT DATE
October 2018

2. REPORT TYPE
Annual

3. DATES COVERED
30 Sep 2017 - 29 Sep 2018

4. TITLE AND SUBTITLE
Integration of the Residual Limb with Prostheses via Direct Skin-Bone-Peripheral Nerve Interface

5a. CONTRACT NUMBER

5b. GRANT NUMBER
W81XWH-16-1-0791

5c. PROGRAM ELEMENT NUMBER

6. AUTHOR(S)
Mark Pitkin

email: mpitkin@tuftsmedicalcenter.org

5d. PROJECT NUMBER

5e. TASK NUMBER

5f. WORK UNIT NUMBER

7. PERFORMING ORGANIZATION NAME(S) AND ADDRESS(ES)
.
Poly-Orth International
Sharon MA 02067-1518

8. PERFORMING ORGANIZATION REPORT NUMBER

9. SPONSORING / MONITORING AGENCY NAME(S) AND ADDRESS(ES)
U.S. Army Medical Research and Materiel Command
Fort Detrick, Maryland 21702-5012

10. SPONSOR/MONITOR'S ACRONYM(S)

11. SPONSOR/MONITOR'S REPORT NUMBER(S)

12. DISTRIBUTION / AVAILABILITY STATEMENT
Approved for Public Release; Distribution Unlimited

13. SUPPLEMENTARY NOTES

14. ABSTRACT
The investigators wish the American Veterans and civilians with amputations can use powered prostheses with direct skeletal attachment and direct bidirectional neural control. Since 2004, their work has been devoted improving a skin-device and bone-device interface. Current research is designed as a translational study to develop Skin and Bone Integrated Pylon with Peripheral Neural Interface (SBIP-PNI) directly attached to the residuum and the powered prosthetic hand with bidirectional control. .

15. SUBJECT TERMS-

NONE LISTED

16. SECURITY CLASSIFICATION OF:			17. LIMITATION OF ABSTRACT	18. NUMBER OF PAGES	19a. NAME OF RESPONSIBLE PERSON
					USAMRMC
a. REPORT	**b. ABSTRACT**	**c. THIS PAGE**			**19b. TELEPHONE NUMBER** *(include area code)*
U	U	U	UU	50	

TABLE OF CONTENTS

1. INTRODUCTION:

The investigators wish the American Veterans and civilians with amputations can use powered prostheses with direct skeletal attachment and direct bidirectional neural control. Since 2004, their work has been devoted improving a skin-device and bone-device interface. Current research is designed as a translational study to develop Skin and Bone Integrated Pylon with Peripheral Neural Interface (SBIP-PNI) directly attached to the residuum and the powered prosthetic hand with bidirectional control.

2. KEYWORDS:

Direct skeletal attachment; powered prosthesis; neural interface; bidirectional control system.

3. ACCOMPLISHMENTS:

What were the major goals of the project?

Goals/Milestones

Year 1

 Manufacture the integrated pylons with peripheral neural interface (SBIP-PNI) for animal studies and fabricate the powered prostheses with sensory feedback

Milestones #1: Meeting the Poly-Orth specification and passing the QC tests – planned in Q2; current completion 100%

Milestone #2: Ship the implants to the Pine Acre Rabbitry/Farm (PARF) and to Georgia Institute of Technology (GIT – – planned in Q2; current completion 100%.

Comment: the site #2 for animal studies with pigs has been changed from PARF to DaVinci Biomedical Research, Lancaster, MA, with corresponding approval.

 Implant SBIP-PNI into cats - planned in Q4; current completion 75%

 Supply cats with powered prostheses with sensory feedback and initiate gait study- planned in Q4: will be completed in Q1 of Year 3

Year 2

 Conclude cat gait study with and without sensory feedback. Will be completed in Q1 of Year 3.

 Implant SBIP-PNI into Yorkshire Swine and conduct gait study with and without sensory feedback: Gait study without sensory feedback completed.

Year 3

 Perform mechanical testing of device skin and device-bone attachment Perform histological analysis of the samples

 Conclude pig gait study with and without sensory feedback

 Demonstrate infection free sustainable device-body interface with the SBIP-PNI

 Demonstrate that adverse events rate (AER) in animal study is lower than the established threshold

 Submit application for IDE to the FDA Comments/Challenges/Issues/Concerns

If the project was not intended to provide training and professional development opportunities or there is nothing significant to report during this reporting period, state "Nothing to Report."

Nothing to Report

How were the results disseminated to communities of interest?
If there is nothing significant to report during this reporting period, state "Nothing to Report."

Describe how the results were disseminated to communities of interest. Include any outreach activities that were undertaken to reach members of communities who are not usually aware of these project activities, for the purpose of enhancing public understanding and increasing interest in learning and careers in science, technology, and the humanities.

Abstracts and Publications

Park H, Islam MS, Grover MA, Klishko AN, Prilutsky BI, DeWeerth SP. A prototype of a neural, powered transtibial prosthesis for the cat: Benchtop characterization. Frontiers in Human Neuroscience. *Frontiers in Neuroscience* **12**: 471, 2018 (attached to this report).

Jarrell J, Farrell BJ, Kistenberg RS, Dalton JF, Pitkin M, Prilutsky BI. Kinetics of individual limbs during level and slope walking with a *unilateral transtibial bone-anchored prosthesis in the cat. Journal of Biomechanics,* ***76****: 74-83, 2018* (attached to this report).

*Park H, Klishko AN, Oh K, Dalton JF, DeWeerth SP, Pitkin M, Prilutsky BI. Cat locomotion with a powered prosthesi*s integrated with residua bone, skin, sensory nerves and muscles. In: Minisymposium of Society for Neuroscience Annual Meeting, San Diego, CA.

What do you plan to do during the next reporting period to accomplish the goals?
If this is the final report, state "Nothing to Report."

Describe briefly what you plan to do during the next reporting period to accomplish the goals and objectives.

In Year 3, we plan

- to complete the study in cats with powered prostheses attached to the residuum via Skin and Bone Integrated Pylon with Peripheral Neural Interface (SBIP-PNI) to demonstrate effectiveness of the neural control in animal gait compared to passive prostheses.
- To complete the study in pigs with the SBIP-PNI to demonstrate safe and sustainable bone-device and skin-device interface.

4. **IMPACT:** Describe distinctive contributions, major accomplishments, innovations, successes, or any change in practice or behavior that has come about as a result of the project relative to:

What was the impact on the development of the principal discipline(s) of the project?
If there is nothing significant to report during this reporting period, state "Nothing to Report."

Describe how findings, results, techniques that were developed or extended, or other products from the project made an impact or are likely to make an impact on the base of knowledge, theory, and research in the principal disciplinary field(s) of the project. Summarize using language that an intelligent lay audience can understand (Scientific American style).

1. Cat study at the Georgia Institute of Technology

In the beginning of the project Year 2 in October 2017, the Georgia Tech group ordered 8 cats from the animal supplier. At that time the available cats were too young to start the study, therefore their arrival was postponed for 7 months. Since receiving animals in late May 2017, the Georgia Tech group trained 4 cats to walk on a walkway and split-belt treadmill, and recorded baseline full-body mechanics of locomotion of these cats prior to implantation surgery. The surgeries were conducted on all 4 cats.

1.1 A prototype of a powered, sensing transtibial prosthesis for cats.

The prosthesis development has included (i) selection of appropriate components (motor, buttery, electronics, stimulator, etc.) that satisfy constraints on the mass of the cat distal leg and ankle power production; (ii) designing electronics, control algorithms, carbon fiber feet and a system for attaching the prosthesis to the percutaneous pylon; (iii) manufacturing parts and integrating them together and (iv) testing (see below).

The diagram illustrating exchange of information between the prosthesis and external devices is depicted in Fig. 1. An MCU CC2510F32 was used to control the wireless communications with the MCU on the prosthesis.

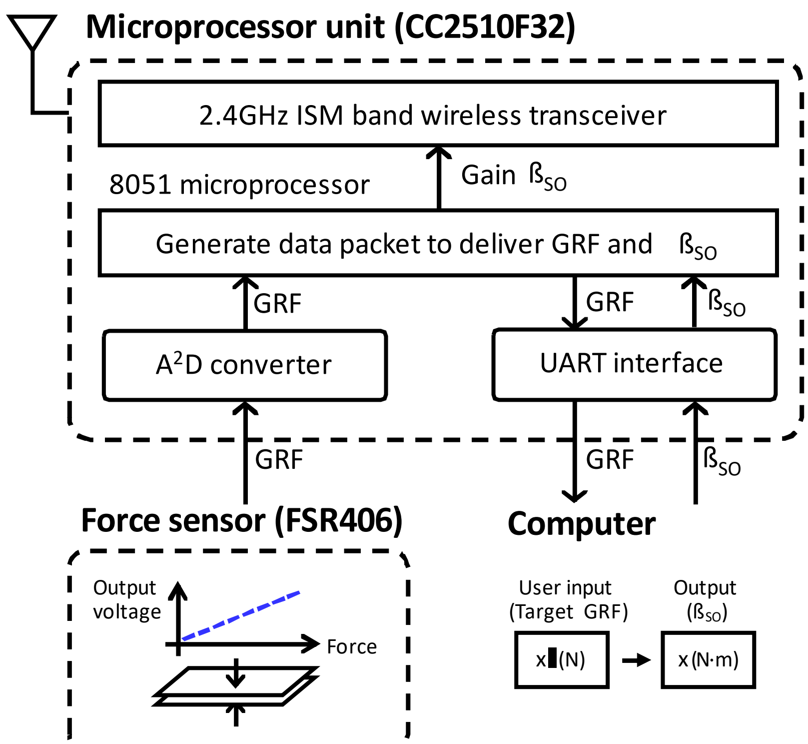

Figure 1. Detailed system block diagram of communications between the prosthesis and external devices (computer, force sensor and microprocessor unit). For details, see text.

A force sensing resistor FSR406 (Interlink electronics, CA, USA) measured ground reaction force exerted by the prosthesis, while a computer monitored the measured ground reaction force in real time and changed the ankle extension gain β_{SO} (see eq. 1 below) by a predefined step magnitude to adjust the peak ground reaction force to the target value. The MCU generated a pulse-width modulated (PWM) output to change the gain β_{SO}.

Based on the operating principle of the DC motor, we assumed that gain β_{SO} was proportional to the duty factor of PWM control signal (Weber et al. 1965). A user set the target gait metric on the computer screen with a LabView (National Instrument, TX, USA) application and β_{SO} was updated every cycle of the gait.

The cat transtibial prosthesis was designed based on the above information. The length of the aluminum rod was set at a half of the shank length, i.e. 55 mm. The linear motor PQ12-63-06-P, Li-polymer battery and other prosthetic components were selected to meet the requirements for the maximum prosthesis mass and moment generation ability. As a result, the prosthesis mass was 80 g and the maximum measured moment during the testing (see below) was 0.6 Nm, which is close to the maximum ankle moment during level walking in the cat.

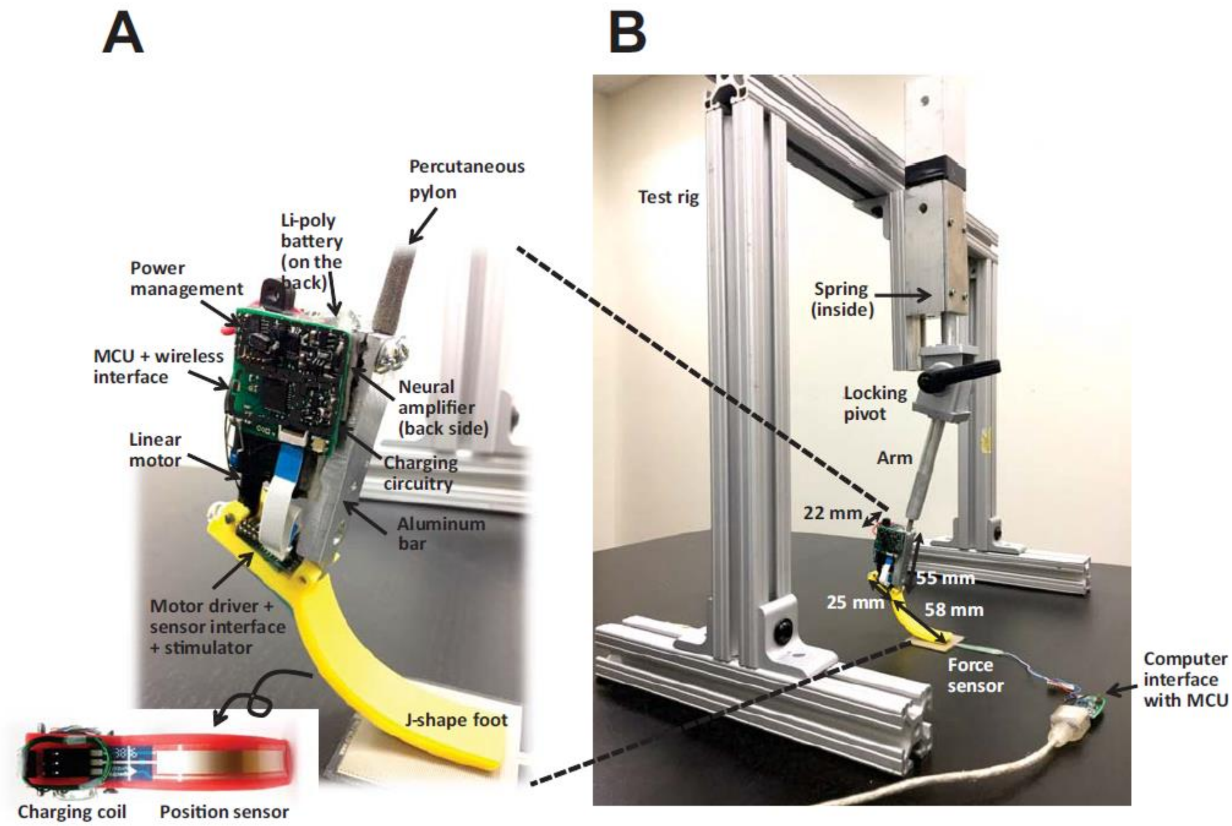

Figure 2. **A**: Prosthesis prototype. **B**: Test rig with the attached prosthesis.

We tested the developed prosthesis and control algorithms in a test rig that held the prosthesis slightly above the ground (Fig. 2B). Previously recorded EMG activity of an ankle extensor SO and and β_{SO} was updated every cycle of the gait.

1.2. Developing passive prosthesis for training to walk with a transtibial prosthesis

A passive prosthetic foot was designed such that it would deflect similarly to the intact limb during stance phase (Gregor et al., 2006). Secondly, the foot must withstand forces applied during normal cat locomotive activities, particularly jumping (4 times body weight, 180 N) (Zajac et al., 1981). Thirdly, the foot should contact the ground at similar orientation to the intact limb and not inhibit walking on slopes up to 50% grade (27°).

Baseline data of the cats prior to amputation was collected in the intact cats prior to surgery and used to develop the prosthetic foot shape. Finite Element Analysis (FEA) models were then used to evaluate shape design. Material properties were determined experimentally by creating test samples and loading them in a single axis loading fixture with a single axis load cell (Chatillon, Amtek) and mechanical dial indicator with 0.0001 inch graduations (M216, Brown & Sharpe). Young's modulus and material density were calculated and fed back into the FEA model.

Different thicknesses and lamination schedules were then reiterated in the FEA models until the stiffness of the foot match the biological system and peak stresses during simulated jumping would not exceed the material's ultimate stress.

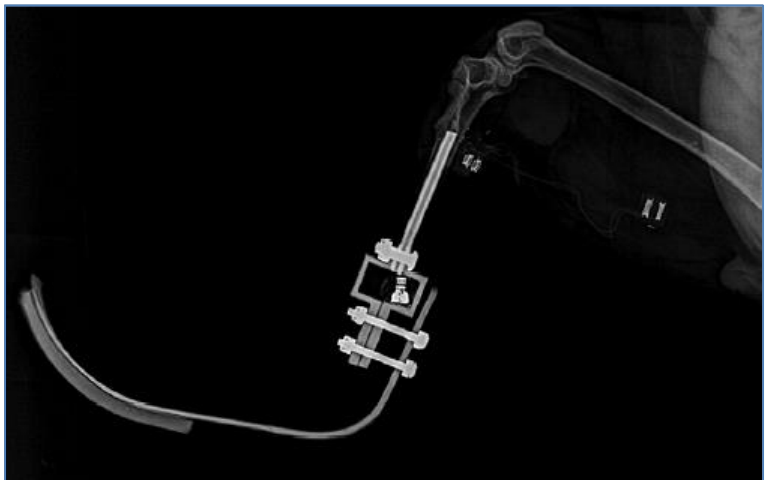

Figure 3. X-ray image of the SBIP-PN implant with attached passive transtibial prosthesis. Nerve cuff electrodes on the distal tibial and sciatic nerves with their leads and leads from muscle electrodes in the residual soleus and tibialis anterior muscles can be seen. The electrode leads were passed through the tibia and implant and secured with a connector in the aluminum chamber. The passive prosthesis can be substituted with a powered one. The connector will be used to transmit myoelectric signals and electrical stimulation trains between the prosthesis and muscles and sensory nerves.

The final design was constructed and loaded to peak predicted forces from cat jumping data using the loading fixture to verify stiffness and ultimate stress of the feet matched the FEA model. carbon fiber laminated with two-part epoxy (West System 105 epoxy with 209 hardener) and cured under vacuum at room temperature for 24 hours; the feet had an average stiffness of 2.02 N/mm and failed at 40N.

The second iteration, a thicker tapered lamination to reinforce the ankle and two layers of nyglass, had an average stiffness of 3.03 N/mm and failed at 95N. A third design iteration used 4 layers of unidirectional fiberglass cloth, 2 layers of 45 x 45 degree of fiberglass cloth, and one layer of 45 x 45 degree 3k carbon fiber with two-part epoxy had an average stiffness of 1.5 N/mm and failed at 60N.

The data from the early failures of the carbon fiber feet were used to better calibrate the FEA models and increase the model's predictive capacity until acceptable feet were produced. FEA models indicated that fiberglass, with a lower young's modulus, would be a more appropriate material for the foot. Three cats were fitted with the designed passive prosthetic feet and were trained to walk for one-four weeks.

All three cats demonstrated reasonable use of the prosthetic limb. Two cats lost their implanted pylon during this training period. One animal has demonstrated good walking and its walking mechanics will be recorded starting in January 2018 before attaching the sensing, powered prosthesis to the residual limb.

1.3. Locomotor training and recordings of the cat with a passive prosthesis

Starting in January 2018, the Georgia Tech team has recorded overground level and slope (±50%) locomotion and treadmill walking of one cat with a passive prosthesis (Fig. 1). During initial recordings of overground locomotion, the cat loaded the prosthetic limb slightly (~30% of the peak ground reaction force produced by the sound contralateral hindlimb).

After ~2 months of training and recordings, the cat started to utilize the passive prosthesis more. Eventually, the peak ground reaction forces achieved ~up to 60-70% of the values observed in the sound hindlimb.

1.3. Improvements in the powered prosthesis

In the period from April to June 2018, the GIT have redesigned and fabricated a new frame for the powered prosthesis that allows for a simple switch between the passive and powered prosthesis without sedating the animal in each experimental session. The new frame design is shown in Fig. 1. The frame is attached to the holder of the percutaneous pylon. The pylon holder includes a box for keeping and protecting the implanted electrodes with the connector. The holder can be attached to passive foot or to the frame with the powered prosthesis by two bolts and nuts. Then the connector from the box is attached to the connector on the powered prosthesis.

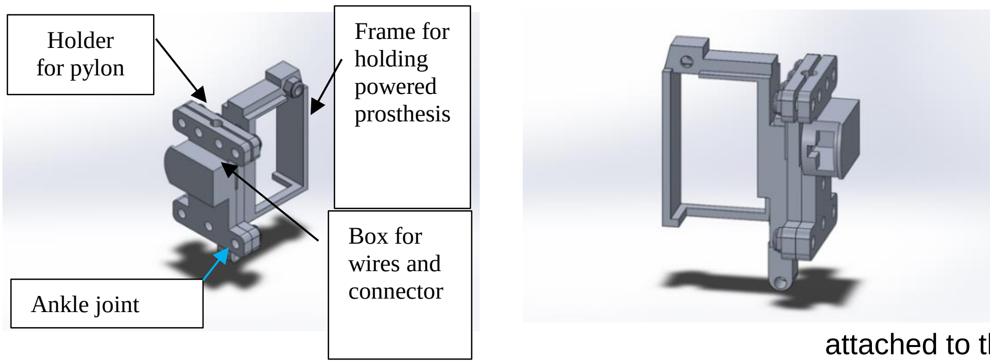

Figure 4. Two views of schematic of the frame for holding the prosthesis. The schematics demonstrates the frame supporting the prosthetic actuator with the circuit board and battery, the two aluminum plates with the opening for holding the pylon implanted to the tibia, and the box for holding the wires from the electrodes and the connector. Note the axis of the prosthetic ankle joint.

The powered prosthesis in the new frame is depicted in Fig. 4. The prosthesis comprised (1) a microprocessor unit (CC2510F32 (Texas instruments, TX, USA), (2) EMG amplifier INA128 with gain of 1000 (V/V) (Texas Instruments, TX, USA), (3) current stimulator with a programmable resistor AD5162 (Analog Devices, MA, USA), (4) ThinPot linear force-position sensor (Spectra Symbol, UT, USA), (5) miniature linear actuator PQ12-63-06-P (Actuonix, BC, Canada), (6) Li-polymer rechargeable battery GM053040 with coil, (7) power management, and (8) prosthetic foot.

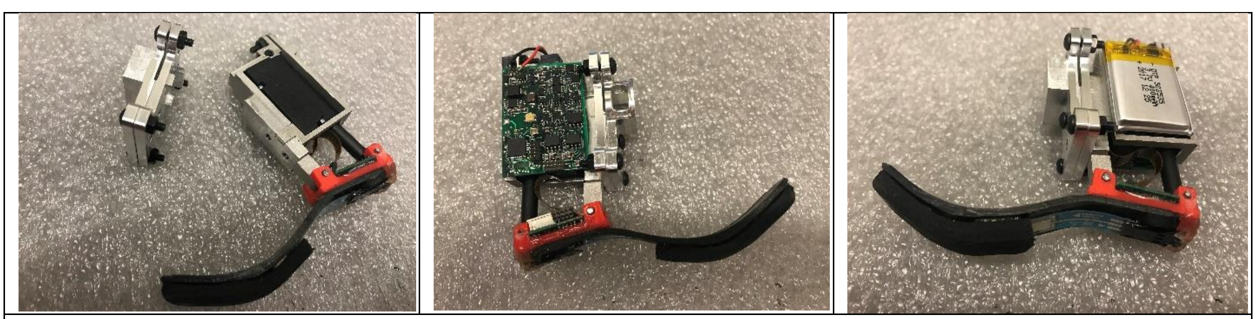

Figure 5. The powered prosthesis inside the holding frame. Left panel demonstrates the pylon holding plates (see Fig. 1) and the frame with a linear actuator and foot attached to the holding plates at the prosthetic joint. Middle panel shows a circuit board fixed to the right side of the linear actuator. The board includes a microprocessor unit, EMG amplifier, current stimulator and power management. Right panel shows the battery attached to the left side of

the actuator. The battery supplies power for the actuator, circuit board with its components and force sensor on the plantar surface of the foot (see right panel).

1.4. Locomotor training and recordings of intact cats

In the period of April – June 2018, the Georgia Tech team has trained the last two intact cats to walk on a walkway and completed recordings of 3D full-body kinematics and ground reaction forces during overground level and slope (±50%) locomotion. These cats are now completing training of walking on a split-belt treadmill. We plan to complete training and recordings of treadmill walking in the end of June – mid July. These cats will be implanted in July or early August.

1.5. Changing surgical implantation strategy

In the latest surgeries, we implanted two cats with the SBIP pylon and nerve and EMG electrodes simultaneously as in all previous cats. To keep the wires secured in case the cats remove the cast, which happened in all previous surgeries, we attached the pylon holder with the box for wires to the implanted pylon. This allowed keeping the wires intact if the cast is removed. However, it turned out that it was impossible to avoid contact between the pylon holder and the cast due to large size of the holder. As a result, any contact of the cast with external environment was directly transmitted to the pylon and prevented its integration with the bone. Because of poor integration, the pylon was pulled out by each cat as soon as the cast was removed and a passive prosthesis attached.

In the next surgeries on the remaining two cats, we will modify the surgical procedures. We will implant the pylon without electrodes and their leads in the first surgery. However, a small bone hole will be drilled and suture inserted inside the pylon and the bone hole. Cast will be placed on the residual limb to protect the implant, as was done in our previous studies. If the cast is removed, it will be replaced within several hours. This procedure permitted good integration of the pylon with bone in the past. After integration is completed (in about 2 months), we will conduct a second surgery, during which nerve cuff and EMG electrodes will be implanted and passed through the bone hole and pylon using the implanted suture. The wires will be secured in the box of the pylon holder (Fig. 1) and a passive prosthesis will be attached to the pylon.

1.6. Determining inertial properties of the passive and powered transtibial prostheses

In order to perform an inverse dynamics analysis of walking with the passive and powered transtibial prostheses, we determined inertial properties of these prostheses using Solidworks (TriMech, LLC). The inertial parameters included the position of the center of mass (COM), mass and moment of inertia in the sagittal plane with respect to the COM of the prosthetic digits, tarsals and shank. The shank segment included the prosthetic components (the aluminum frame, actuator, battery, porous titanium implant) and the intact proximal portion of the shank.

The obtained inertial parameters for the passive prosthesis are as follows: COM position in the sagittal YX plane with respect to the proximal end of the implant (Point 1, Fig. 1) is Y=-82.55 mm, Z=23.54 mm; mass is 37.42 g; and principal moment of inertia with respect to the X axis is Ix=13824.24 g*mm^2.

Similar calculations were performed for the powered transtibial prosthesis separately for the prosthetic digits, tarsals and shank with a portion of the residual shank (Fig. 2). Calculations yielded the following inertial properties for the digits (Fig. 2A): COM location in the sagittal XZ plane with respect to the proximal (right) end of the segment is X=22.81 mm, Z=-4.33 mm; mass is 6.61 g; and principal moment of inertia with respect to the Y axis is Iy=1238.21 g*mm^2.

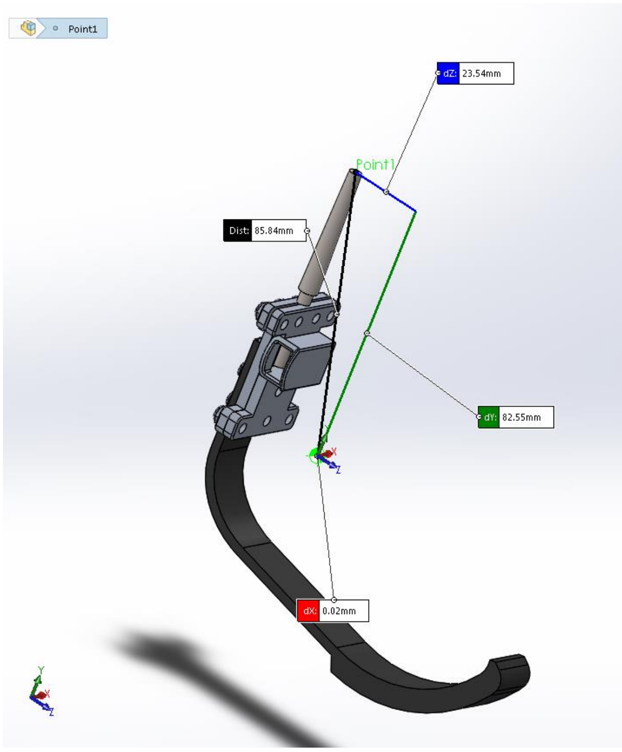

Figure 1. COM location and coordinate frames of passive transtibial prosthesis

For the prosthetic tarsals (Fig. 2B) the inertial parameters are: COM location in the sagittal XZ plane with respect to the proximal (right) end of the segment is X=45.26 mm, Z=-6.09 mm; mass is 5.99 g; and principal moment of inertia with respect to the Y axis is Iy=3540.13 g*mm^2.

For the prosthetic shank with the residual shank (Fig. 2C) the inertial parameters are: COM location in the sagittal XY plane with respect to the proximal (right) end of the segment is X=53.64 mm, Y=0.02 mm; mass is 106.38 g; and principal moment of inertia with respect to the Z axis is Iz=95178.15 g*mm^2.

Ankle angle and ground reaction forces during locomotion with a transtibial powered prosthesis

In the period from June through September 2018, we have recorded level walking of the cat with the powered transtibial prosthesis. The prosthesis design allows for two modes of the actuator

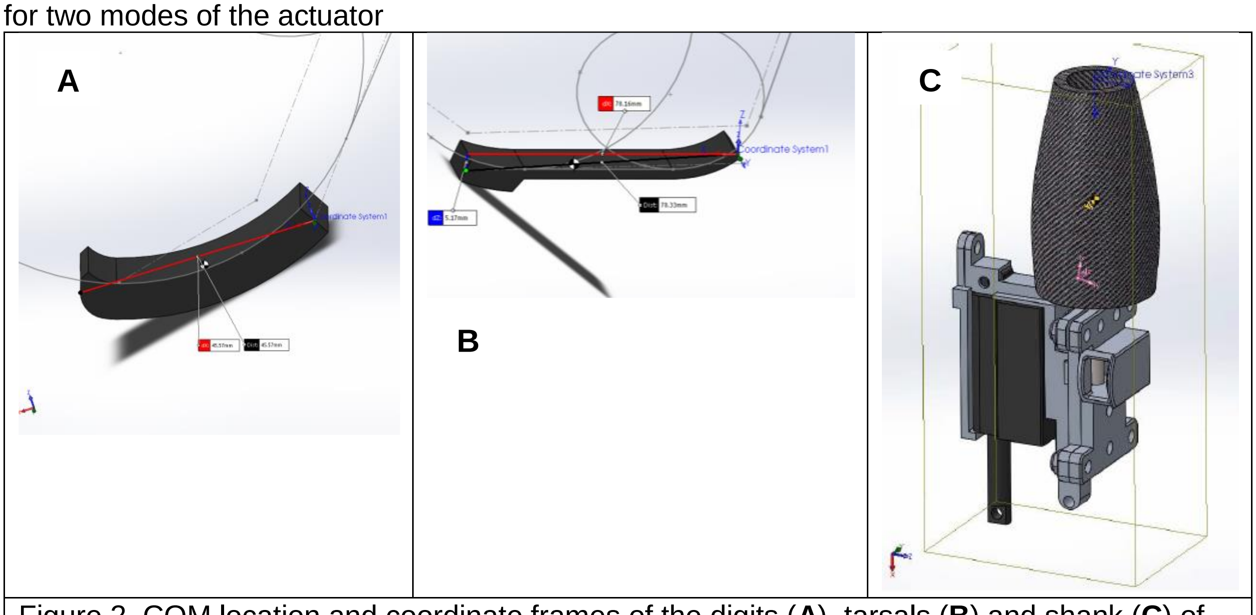

Figure 2. COM location and coordinate frames of the digits (**A**), tarsals (**B**) and shank (**C**) of the powered transtibial prosthesis

control. In the first mode, the actuator ankle extension is triggered by contact of the foot with the ground and flexion, by unloading the foot. In the second mode, ankle extension is triggered by EMG signal from a residual ankle extensor and ground contact, whereas ankle flexion is again triggered by unloading the foot. So far we have tested the first mode of actuator control to establish the best actuator in terms of its gear ratio: 30, 63 and 100.

Ankle angle

Comparisons of ankle angles during intact walking and walking with the powered transtibial prosthesis with gear ratios 30, 63 and 100 are shown in Fig. 3. In all gear ratios the initial and final ankle angles were much lower than in intact walking (100-115 deg vs 140-155 deg). The ranges of ankle flexion in swing and extension in stance were also much smaller in the prosthetic joint (~12-20 deg) than in intact one (40-50 deg).

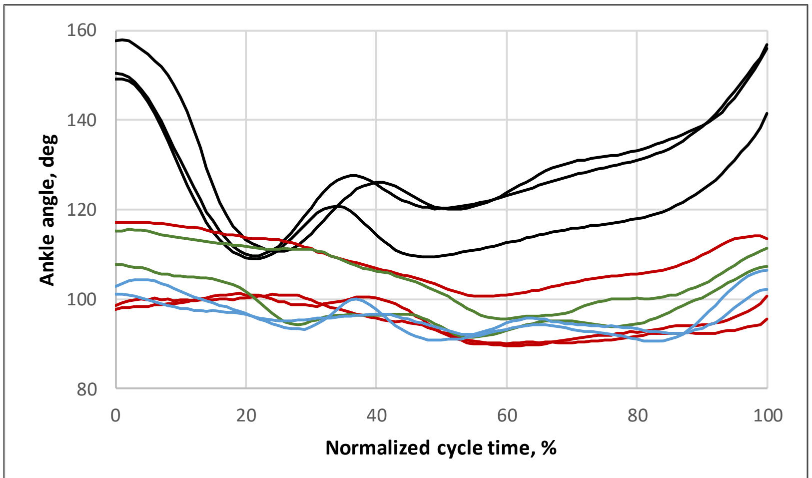

Figure 3. Ankle angles of representative cycles of one cat during level walking before amputation (black lines) and with powered transtibial prostheses with gear ratio 30 (blue lines), 63 (green lines) and 100 (brown lines). Cycle starts with swing onset, stance starts at ~35-40% in intact walking and at ~50-55% in prosthetic walking.

Ground reaction forces

The peak magnitude of the vertical forces during prosthetic walking was about the same as during intact one (~17 N; Fig. 4).

However, the duty factor, i.e. the relative duration of the stance phase in the cycle was smaller during prosthetic walking (~50% vs ~70% in intact walking). The anterior forces were

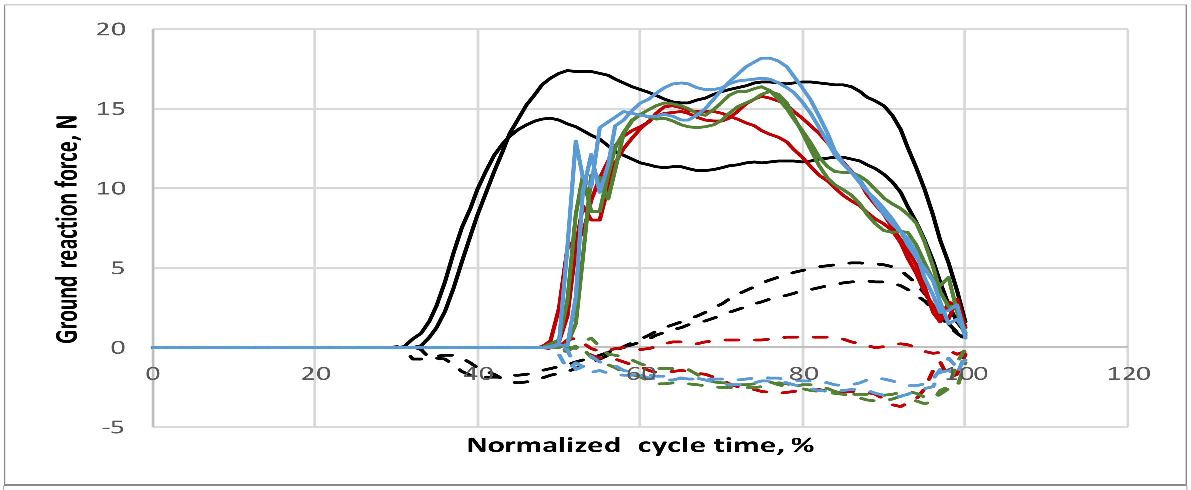

Figure 5. Figure 4. Vertical (continues lines) and anterior-posterior (dashed lines) ground reaction forces of representative cycles of one cat during level walking before amputation (black lines) and with powered transtibial prostheses with gear ratio 30 (blue lines), 63 (green lines) and 100 (brown lines).

typically negative during the entire stance during prosthetic walking, i.e. prosthetic limb did not generate propulsive forces in the forward direction. There was no difference in the magnitude and pattern of the vertical and anterior-posterior forces between different gear ratios.

Pig study at DaVinci Biomedical

1 Study design

The gait study population consisted of one (1) animal. The animal was prepared in a sterile OR, sedated and underwent transtibial amputation. After the amputation, the SBIP-PNI was implanted directly into the distal tibial segment. The animal was recovered, received post-operative care with monitoring and pain medication. The animal was survived for 89 days.

A baseline, post prosthesis weight load, and pre-sacrifice gait assessment were performed by the client. General implant tissue assessments were made as part of the daily clinical and health assessment. Baseline, 3 weeks, and pre-sacrifice imaging was performed along with clinical pathology health analysis.

At the end of the survival, a gross examination was performed of the implant site and the implant with the surrounding tissue harvested for mechanical testing.

2 Results

Post-Operative Evaluations

The animal recovered well from the amputation and implant surgery. During the survival period it healed normally without any complications. On Day 13, a culture and sensitivity was taken on the implant site. The bacteria recovered were sensitive to the antibiotics already being administered (Ceftiofur and Enrofloxacin). The antibiotics were given throughout the survival period on a weekly basis. The bandage/aluminum support was monitored twice daily at a minimum and changed as needed, beyond the scheduled timepoints.

Procedure Date	Day	Body Condition score	Comments / Notes
8/1/17	-1		Gait analysis pre-implant surgery
8/2/17	0	5/9	Surgery to implant device 75 mg/hr Fentanyl patch applied at 0615. Procedure start time 0714. Marked the incision outline - first incision, disarticulated tibia from metatarsals - also removed distal aspect of the fibula. Drilled medullary cavity, followed by reamer. Bacitracin 9.8 mL irrigated into amputation site prior to implant placement at 0900. Placed device into medullary cavity at distal end of tibia. Placed skin flap over post. Fluoroscopy post-op. Placed aluminum prosthetic support. Recovered animal.
8/2/17	0	5/9	Sedation for bandage change/repair at ~1400. Cleaned incision/implant site. Replaced aluminum support.
8/7/17	5	5/9	Incision healing well/normal. Inflammation: incisional and around implant. No odor. Granulation tissue around implant. Cleaned implant with betadine. Rewrapped with roll cotton and Elasticon. Placed aluminum support over implant and distal tissue - wrapped with Elasticon, sutured to skin.

8/15/17	13	3/9	Granulation tissue around implant. Sutures removed. Slight odor, dehiscence of anterior aspect near implant. No attachment to implant. Excede and Baytril given IM at 10:33. Culture taken of implant/SC interface. Fluoroscopy performed. Rebandaged.
8/23/17	21	5/9	Tissue at implant transition area is granulated and healing. Mild inflammation. Normal bandage change. No abnormalities, tissue is contracting around implant.
8/30/17	28	4/9	Bandage change, healing: granulation tissue at implant site moderate. Inflammation: irritation of posterior stifle due to pressure of cup against leg. Repairs / Interventions: recovered implant site post removal of scabs at distal aspect. Abnormalities: none Not painful, will place splinted leg down.
9/1/17	30	NA	Bandage repair. Implant site scabbed over. Replaced bandage and splint.
9/6/17	35	NA	Distal aspect of amputation site healthy, granulation tissue, loose at implant, not odiferous - cleaned and rebandaged. Fluoroscopy: Bony callous on fibula, new bone growth (callous) at distal aspect of tibia.
9/14/17	43	3/9	Removed dried discharge from around implant. Healthy granulation tissue, no odor. Fluoroscopy: bony callous.
9/15/17	44	NA	Bandage repair.
9/21/17	50	3/9	Granulation tissue at distal amputation site around implant. Fluoroscopy- normal healing. Serosanguinous discharge around implant site, removed and sprayed with Prepodyne. Joint angle 137□
9/27/17	56	2.5/9	Granulation tissue at distal aspect
10/4/17	63	2.5/10	1. Healthy granulation tissue, minimal inflammation. Prosthesis was placed onto implant. 2. Prosthesis had fallen off at about 1PM. @~15:00 attachment of a modified prosthesis was attempted but further modifications needed. Animal was bandaged and recovered.
10/9/17	68		Gait analysis 3-leg
10/10/17	69		Gait analysis peg leg prosthetic version 1
10/10/17	69	3/9	1. Prosthetic placed (DaVINCI I), a small amount of exudate was present at prosthesis/skin transition area. 2. At ~1600 PM gait assessment performed. Animal walked on walkway, learning to use the prosthetic device. A video was obtained. A follow-up gait analysis will be performed in approximately a week.

Procedure Date	Day	Body Condition score	Comments / Notes
10/12/17	71	2.5/9	Modification to the prosthetic post.
10/16/17	75	2.5/9	New prosthesis attached (DaVINCI II). Mostly granulation tissue at distal end.
10/17/17	76	NA	Shortened length of prothesis ~ 1.25" (by DaVINCI)
10/18/17	77	NA	Gait analysis peg leg prosthetic version 2
10/23/17	82	NA	Gait analysis C shaped prosthetic version 3
10/30/17	89	2.5/9	Animal was euthanized

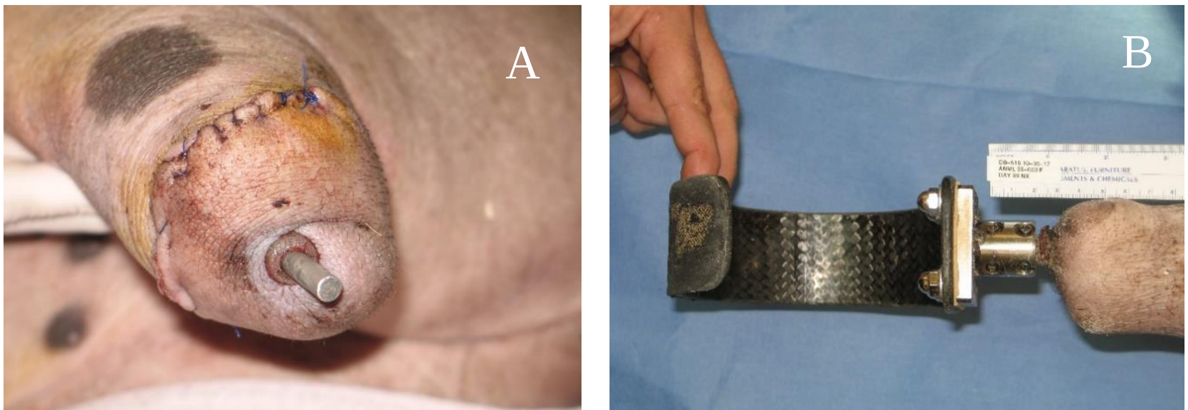

Figure 1. Implantation site. **A** - day of the surgery; **B** - day 89 with attached prosthesis.

Fluoroscopy Imaging

Fluoroscopic imaging was used to monitor bone to device interface. The device remained stable within the medullary cavity throughout the survival period. Bone callous formed at the distal end of the tibia and fibula, as would be expected.

Baseline

Day 0: post-Implant

	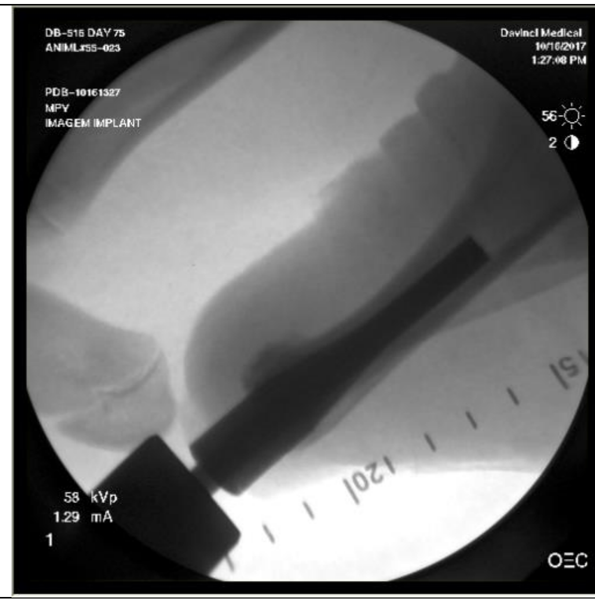
Day 56	Day 75

Gait Evaluation

Gait Evaluation Date	Gait Analysis Day	Comments
8/1/17	-1	Gait analysis pre-implant surgery
10/9/17	68	Gait analysis 3-leg
10/10/17	69	Test peg leg prosthetic version 1
10/18/17	77	Test peg leg prosthetic version 2
10/23/17	82	Test C-shaped prosthetic version 3
10/30/17	89	Data collection with Gait Analysis

Gait analysis

Gait analysis was performed before the implantation procedure and at Day 82 following implantation.

Three different prosthetic devices were fabricated and tested. A C-shape prosthesis (**Fig. 1., B**) was selected for the gait study due to its durability, light weight and springiness well accepted by the subject animal (**Fig. 3**).

Figure 2. Animal with C-Prosthesis

The *Strideway* Gait Analysis System, Tekscan, Inc., Boston, MA, was used for collection of ground reactions and kinematic parameters in a free gait of the animal (**Fig. 3**).

Results

Figure 2. Setting for gait analysis. **1**- instrumented walkway; **2** – entrance to the site; **3** – exit from the site.

Criterion of acceptance of the prostheses attached to the implanted SBIP pylon is a symmetry of maximal loads on both hid legs. According to the Symmetry table below, the index of symmetry for the stance time was 0.90, and for the max ground reaction force was 0.86.

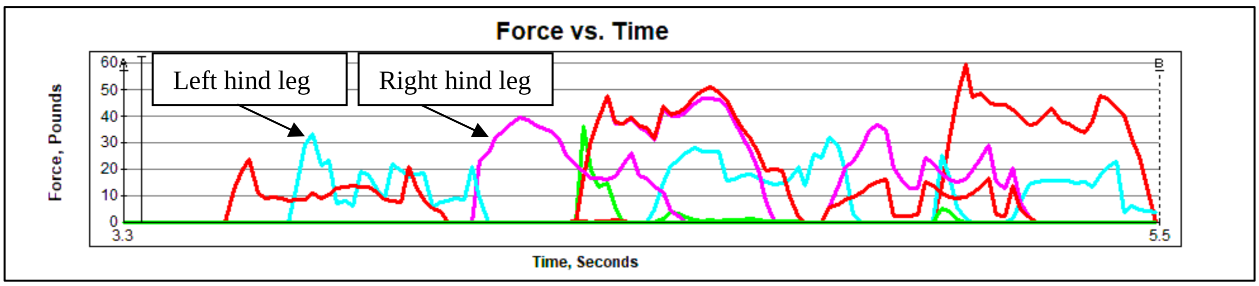

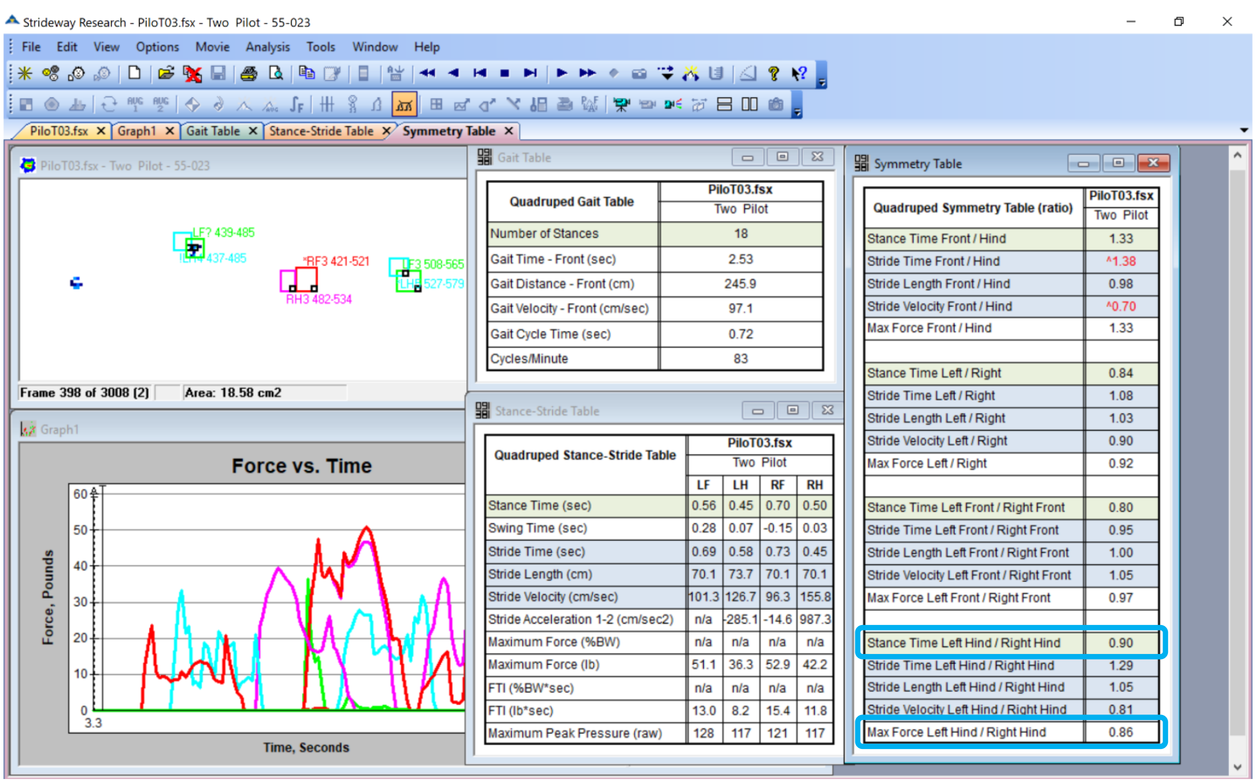

Quadruped Gait Table	PiloT03.fsx Two Pilot
Number of Stances	18
Gait Time - Front (sec)	2.53
Gait Distance - Front (cm)	245.9
Gait Velocity - Front (cm/sec)	97.1
Gait Cycle Time (sec)	0.72
Cycles/Minute	83

Quadruped Stance-Stride Table	PiloT03.fsx Two Pilot			
	LF	LH	RF	RH
Stance Time (sec)	0.56	0.45	0.70	0.50
Swing Time (sec)	0.28	0.07	-0.15	0.03
Stride Time (sec)	0.69	0.58	0.73	0.45
Stride Length (cm)	70.1	73.7	70.1	70.1
Stride Velocity (cm/sec)	101.3	126.7	96.3	155.8
Stride Acceleration 1-2 (cm/sec2)	n/a	-285.1	-14.6	987.3
Maximum Force (%BW)	n/a	n/a	n/a	n/a
Maximum Force (lb)	51.1	36.3	52.9	42.2
FTI (%BW*sec)	n/a	n/a	n/a	n/a
FTI (lb*sec)	13.0	8.2	15.4	11.8
Maximum Peak Pressure (raw)	128	117	121	117

Quadruped Symmetry Table (ratio)	PiloT03.fsx Two Pilot
Stance Time Front / Hind	1.33
Stride Time Front / Hind	^1.38
Stride Length Front / Hind	0.98
Stride Velocity Front / Hind	^0.70
Max Force Front / Hind	1.33
Stance Time Left / Right	0.84
Stride Time Left / Right	1.08
Stride Length Left / Right	1.03
Stride Velocity Left / Right	0.90
Max Force Left / Right	0.92
Stance Time Left Front / Right Front	0.80
Stride Time Left Front / Right Front	0.95
Stride Length Left Front / Right Front	1.00
Stride Velocity Left Front / Right Front	1.05
Max Force Left Front / Right Front	0.97
Stance Time Left Hind / Right Hind	0.90
Stride Time Left Hind / Right Hind	1.29
Stride Length Left Hind / Right Hind	1.05
Stride Velocity Left Hind / Right Hind	0.81
Max Force Left Hind / Right Hind	0.86

Mechanical tests on bone-implant attachment

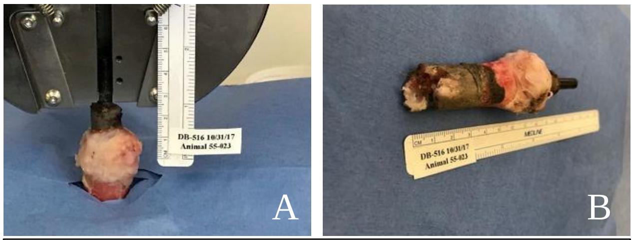

Figure 3. Mechanical Test. **A -** Pull-out test set up. **B** - Failure Mode: Bone fractured at holding pins. Implant to bone interface remained intact.

Rate 1 (mm/min)	Maximum Load (N)	Extension at Maximum Load (mm)
6	5383.7	4.42

DB-516 Pull Out test with 30KN load cell
Temperature 74F
30 KN load cell
Instron Testing Station DaVinci #00316
Tested by Leo Cappabianca, MS
Test Date = 10/31/17

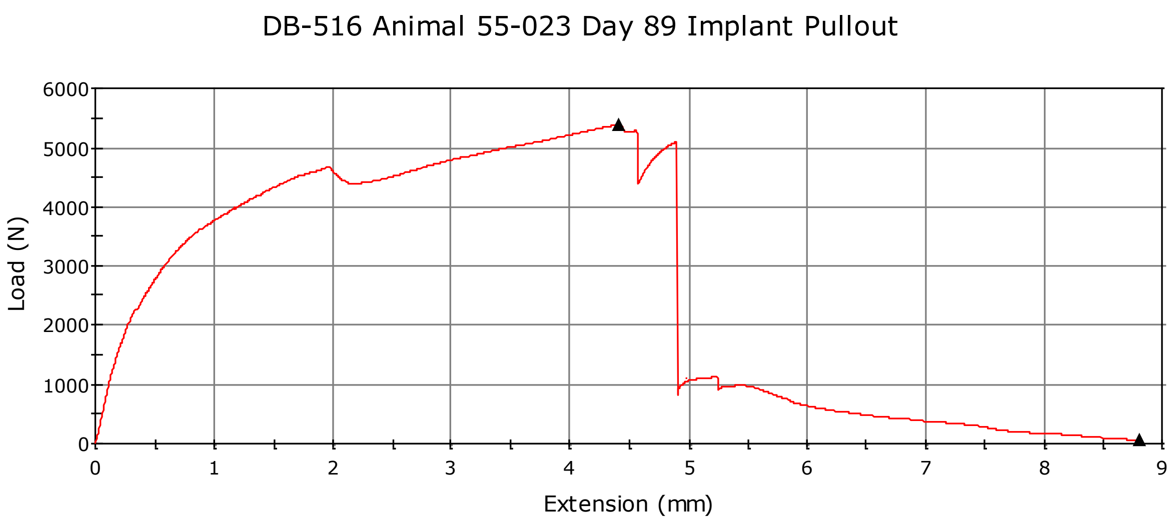

Residuum skin mobility and improvements in the implantation technique.

With positive outcomes in investigating the bone-implant bond, a problem with skin-implant interface in the pig model is still present. The investigators concluded that compared to the cat model successfully used by the colleagues at Georgia Tech, the pig model required further development.

The modifications being approved by ACURO included:

- Investigating a two-stage procedure: 1- amputation; 2 – implantation following a two-months healing period. The purpose is to reduce a volume of swelling prior implantation to mitigate travel of the skin along the pylon missing the porous cladding.
- Using a firm cast to exclude flexing the joint above the residuum. The purpose is to create better conditions for skin ingrowth to the porous cladding during the first two-three weeks after implantation by avoiding movements of the residuum skin along the implant.
- Implanting into the fore limb. Purpose is to allow for safe and reliable immobilization of the residuum and the joint above it.

Preparations for the fore leg implantation

1. Fabrication of new SBIP-PNI pylons with elongated porous cladding

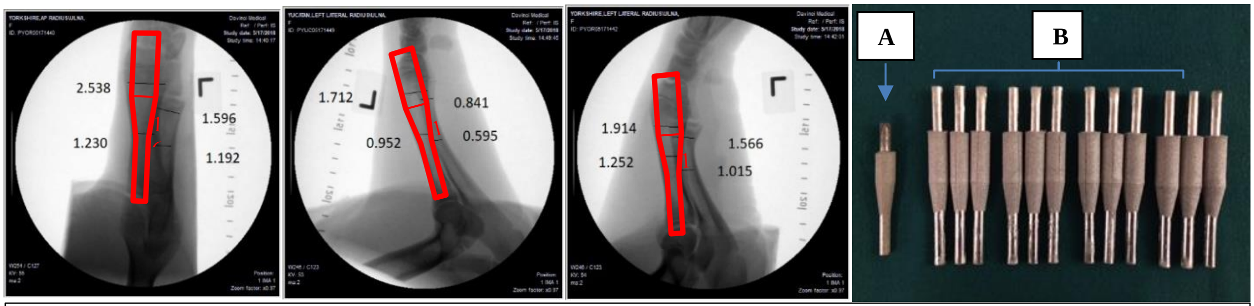

Figure 3. A fore limb implant dimensions and sizing. **A** - initial design SBIP-PNI; **B** - new SBIP-PNI pylons with elongated porous cladding.

2. Two-stage procedure for a fore limb

Figure 4. Healed residuum.

Figure 5. Completion of implantation.

One animal was implanted in the forelimb with the two-stage procedure (**Figs 5-6**). The device insertion depth was controlled to keep the swollen portion of the epithelium against the porous cladding.

3. Development of the implants with oval cross-section

Figure 5. Development of an implant with oval shape to fi to the oval bone canal of a fore limb.

First study with a fore limb implantation showed that the implants with the circular cross-sections might require too much bone to be removed from the marrow canal. That is due to typical and distinct oval shape of the fore limb bone in pigs. Reaming such oval canal by a cylindrical device results in substantial thinning of the bone walls in the direction of a shorter diameter of the cross-section.

In Year 3 we plan to fabricate and test the conical implants of oval shape with better fit to the marrow canal (Figure 5).

What was the impact on other disciplines?

If there is nothing significant to report during this reporting period, state “Nothing to Report.”

Describe how the findings, results, or techniques that were developed or improved, or other products from the project made an impact or are likely to make an impact on other disciplines.

Nothing to report for Year 2.

What was the impact on technology transfer?
If there is nothing significant to report during this reporting period, state "Nothing to Report."
Describe ways in which the project made an impact, or is likely to make an impact, on commercial technology or public use, including:

- *transfer of results to entities in government or industry;*
- *instances where the research has led to the initiation of a start-up company; or*
- *adoption of new practices.*

Nothing to report for Year 2 Recommendations for implantation of the pylons with peripheral neural interface and on bidirectional control of powered prostheses are anticipated at the completion of the project.

What was the impact on society beyond science and technology?
If there is nothing significant to report during this reporting period, state "Nothing to Report."
Describe how results from the project made an impact, or are likely to make an impact, beyond the bounds of science, engineering, and the academic world on areas such as:

- *improving public knowledge, attitudes, skills, and abilities;*
- *changing behavior, practices, decision making, policies (including regulatory policies), or social actions; or*
- *improving social, economic, civic, or environmental conditions.*

The investigators wish the American Veterans and civilians with amputations can use powered prostheses with direct skeletal attachment and direct bidirectional neural control, which could improve the quality of life and social integration of the patients.

5. CHANGES/PROBLEMS: The Project Director/Principal Investigator (PD/PI) is reminded that the recipient organization is required to obtain prior written approval from the awarding agency Grants Officer whenever there are significant changes in the project or its direction. If not previously reported in writing, provide the following additional information or state, "Nothing to Report," if applicable:

Nothing to report

Changes in approach and reasons for change
Describe any changes in approach during the reporting period and reasons for these changes. Remember that significant changes in objectives and scope require prior approval of the agency.

Nothing to report

Actual or anticipated problems or delays and actions or plans to resolve them

Describe problems or delays encountered during the reporting period and actions or plans to resolve them.

1. **Cat study**

Despite delays in delivery and longer acclimation of the cats, last 2 cats will be taken for surgery in Q1 of Year 3.

2. **Pig study**

To address possible tissues swelling after implantation procedure, we plan in Year 3:

- Investigating a two-stage procedure: 1- amputation; 2 – implantation following a two-months healing period. The purpose is to reduce a volume of swelling prior implantation to mitigate travel of the skin along the pylon missing the porous cladding.
- Using a firm cast to exclude flexing the joint above the residuum. The purpose is to create better conditions for skin ingrowth to the porous cladding during the first two-three weeks after implantation by avoiding movements of the residuum skin along the implant.
- Implanting into the fore limb. Purpose is to allow for safe and reliable immobilization of the residuum and the joint above it.

Changes that had a significant impact on expenditures

Describe changes during the reporting period that may have had a significant impact on expenditures, for example, delays in hiring staff or favorable developments that enable meeting objectives at less cost than anticipated.

Nothing to Report

Significant changes in use or care of human subjects, vertebrate animals, biohazards, and/or select agents

Describe significant deviations, unexpected outcomes, or changes in approved protocols for the use or care of human subjects, vertebrate animals, biohazards, and/or select agents during the reporting period. If required, were these changes approved by the applicable institution committee (or equivalent) and reported to the agency? Also specify the applicable Institutional Review Board/Institutional Animal Care and Use Committee approval dates.

Significant changes in use or care of human subjects

N/A

Significant changes in use or care of vertebrate animals.

All modifications in pig study hasvebeen approved by ACURO.

Significant changes in use of biohazards and/or select agents

N/A

6. PRODUCTS: List any products resulting from the project during the reporting period. If there is nothing to report under a particular item, state "Nothing to Report."

- **Publications, conference papers, and presentations**
  Report only the major publication(s) resulting from the work under this award.

  Journal publications. *List peer-reviewed articles or papers appearing in scientific, technical, or professional journals. Identify for each publication: Author(s); title; journal; volume: year; page numbers; status of publication (published; accepted, awaiting publication; submitted, under review; other); acknowledgement of federal support (yes/no).*

Park H, Islam MS, Grover MA, Klishko AN, Prilutsky BI, DeWeerth SP. A prototype of a neural, powered transtibial prosthesis for the cat: Benchtop characterization. Frontiers in Human Neuroscience. *Frontiers in Neuroscience* **12**: 471, 2018 (attached to this report).

Jarrell J, Farrell BJ, Kistenberg RS, Dalton JF, Pitkin M, Prilutsky BI. Kinetics of individual limbs during level and slope walking with a *unilateral transtibial bone-anchored prosthesis in the cat. Journal of Biomechanics,* ***76****: 74-83, 2018* (attached to this report).

*Park H, Klishko AN, Oh K, Dalton JF, DeWeerth SP, Pitkin M, Prilutsky BI. Cat locomotion with a powered prosthesi*s integrated with residua bone, skin, sensory nerves and muscles. In: Minisymposium of Society for Neuroscience Annual Meeting, San Diego, CA.

Books or other non-periodical, one-time publications. *Report any book, monograph, dissertation, abstract, or the like published as or in a separate publication, rather than a periodical or series. Include any significant publication in the proceedings of a one-time conference or in the report of a one-time study, commission, or the like. Identify for each one-time publication: Author(s); title; editor; title of collection, if applicable; bibliographic information; year; type of publication (e.g., book, thesis or dissertation); status of publication (published; accepted, awaiting publication; submitted, under review; other); acknowledgement of federal support (yes/no).*

Nothing to report

Other publications, conference papers, and presentations. *Identify any other publications, conference papers and/or presentations not reported above. Specify the status of the publication as noted above. List presentations made during the last year* *(international, national, local societies, military meetings, etc.). Use an asterisk (*) if presentation produced a manuscript.*

*Park H, Klishko AN, Oh K, Dalton JF, DeWeerth SP, Pitkin M, Prilutsky BI. Cat locomotion with a powered prosthesi*s integrated with residua bone, skin, sensory nerves and muscles. In: Minisymposium of Society for Neuroscience Annual Meeting, San Diego, CA.

- **Website(s) or other Internet site(s)**
  List the URL for any Internet site(s) that disseminates the results of the research activities. A short description of each site should be provided. It is not necessary to include the publications already specified above in this section.

Nothing to report

- **Technologies or techniques**
  Identify technologies or techniques that resulted from the research activities. In addition to a description of the technologies or techniques, describe how they will be shared.

Nothing to report

- **Inventions, patent applications, and/or licenses**
  Identify inventions, patent applications with date, and/or licenses that have resulted from the research. State whether an application is provisional or non-provisional and indicate the application number. Submission of this information as part of an interim research performance progress report is not a substitute for any other invention reporting required under the terms and conditions of an award.

Nothing to report

- **Other Products**
  Identify any other reportable outcomes that were developed under this project. Reportable outcomes are defined as a research result that is or relates to a product, scientific advance, or research tool that makes a meaningful contribution toward the understanding, prevention, diagnosis, prognosis, treatment, and/or rehabilitation of a disease, injury or condition, or to improve the quality of life. Examples include:
  - *data or databases;*
  - *biospecimen collections;*
  - *audio or video products;*
  - *software;*
  - *models;*
  - *educational aids or curricula;*
  - *instruments or equipment;*
  - *research material (e.g., Germplasm; cell lines, DNA probes, animal models);*

- *clinical interventions;*
- *new business creation; and*
- *other.*

Nothing to report

7. PARTICIPANTS & OTHER COLLABORATING ORGANIZATIONS

What individuals have worked on the project?

Provide the following information for: (1) PDs/PIs; and (2) each person who has worked at least one person month per year on the project during the reporting period, regardless of the source of compensation (a person month equals approximately 160 hours of effort). If information is unchanged from a previous submission, provide the name only and indicate "no change."

Name: *Mark Pitkin*
Project Role: *PI*
Researcher Identifier (e.g. ORCID ID): L-7934-2017
Nearest person month worked: *5*
Contribution to Project: *Dr. Pitkin has directed all aspects of the project*
Name: *Grigory Raykhtsaum*
Project Role: *Director of Engineering*
Nearest person month worked: *3*
Contribution to Project: *Mr. Raykhtsaum was responsible for development and manufacturing of the SBIP-PNI pylons for animal studies*
Name: *Charles Cassidy*
Project Role: *Investigator*
Nearest person month worked: *0.1*
Contribution to Project: *Dr. Cassidy is a surgeon on the project performing two procedures in Year I.*
Name: *Boris Prilutsky*
Project Role: *Director of the Georgia Tech study*
Nearest person month worked: *1*
Contribution to Project: *Dr. Prilutsky has directed development of the powered prosthesis for animal studies and the animal trials with SBIP-PNI in Year I.*
Name: *Hangue Park*
Project Role: *Investigator/Postgraduate student of Georgia Tech*
Nearest person month worked: *10*
Contribution to Project: *Dr. Park developed the powered prosthesis for animal studies.*

Has there been a change in the active other support of the PD/PI(s) or senior/key personnel since the last reporting period?
If there is nothing significant to report during this reporting period, state "Nothing to Report."

If the active support has changed for the PD/PI(s) or senior/key personnel, then describe what the change has been. Changes may occur, for example, if a previously active grant has closed and/or if a previously pending grant is now active. Annotate this information so it is clear what has changed from the previous submission. Submission of other support information is not necessary for pending changes or for changes in the level of effort for active support reported previously. The awarding agency may require prior written approval if a change in active other support significantly impacts the effort on the project that is the subject of the project report.

New active support

Mark Pitkin, PI

a) Title of the project: R44 HD 090768 Large animal study on deeply porous transcutaneous pylon for direct skeletal attachment
b) Funding agency: NIH NCMRR
c) Project period: 09/26/2016 – 08/31/2018
d) Level (%) of effort in the project: 50%
e) Program Official: Louis A Quatrano
Email: quatranl@mail.nih.gov
f) The project is to develop and test new pylons and their implantation technique for direct skeletal attachment of leg prostheses. The goals are to increase integration of the pylons with skin and bone by developing new porous claddings with deep porosity and with Nano silver coating, developing technique of distraction implantation of pylons with side elements, and testing the Rolling Joint Foot and Ankle prosthesis with anticipation of minimizing bending moments from the pylon to the hosting bone.
g) There is no overlap with our current project

Grigory Raykhtsaum, Investigator/Director of Engineering

a) Title: R44 HD 090768 Large animal study on deeply porous transcutaneous pylon for direct skeletal attachment
b) Funding agency: NIH NCMRR
c) PI: Mark Pitkin
d) Project period: 09/26/2016 – 08/31/2018
e) Level (%) of effort in the project: 17%

Boris Prilutsky, PD for Georgia Tech study

a) Title: R01NS100928 Neural mechanisms of locomotion evoked by epidural stimulation of the spinal cord
b) Agency: NIH/NINDS
c) PI: Boris Prilutsky
d) Project Period: 07/15/2017-05/31/2022
e) Level of support: .12%
f) There is no overlap with our current project

What other organizations were involved as partners?
If there is nothing significant to report during this reporting period, state "Nothing to Report."

Describe partner organizations – academic institutions, other nonprofits, industrial or commercial firms, state or local governments, schools or school systems, or other organizations (foreign or domestic) – that were involved with the project. Partner organizations may have provided financial or in-kind support, supplied facilities or equipment, collaborated in the research, exchanged personnel, or otherwise contributed.

1. DaVinci Biomedical Research, 20 Maple St, Lancaster, MA 01523
   - *Financial support: MR150015 Integration of the Residual Limb with Prostheses via Direct Skin-Bone-Peripheral Nerve Interface*
   - *Facilities and personnel collaborating on animal studies with pigs.*
2. Advanced Manufacturing Products (ADMA), Hudson, OH
   - *Financial support: MR150015 Integration of the Residual Limb with Prostheses via Direct Skin-Bone-Peripheral Nerve Interface*
   - *Facilities and personnel for sintering titanium SBIP-PNI pylons with selected specifications for animal studies*
3. Georgia Institute of Technology, Atlanta, GA
   - *Financial support: MR150015 Integration of the Residual Limb with Prostheses via Direct Skin-Bone-Peripheral Nerve Interface*
   - *Conducting animals study with cats wearing powered prostheses following DSA*
4. T3 Labs, Atlanta, GA 30313
   - *Financial support: MR150015 Integration of the Residual Limb with Prostheses via Direct Skin-Bone-Peripheral Nerve Interface*
   - *Facilities and personnel collaborating on animal studies with cats.*

8

COLLABORATIVE AWARDS:

Nothing to report

QUAD CHARTS:

9. APPENDICES: Attach all appendices that contain information that supplements, clarifies or supports the text. Examples include original copies of journal articles, reprints of manuscripts and abstracts, a curriculum vitae, patent applications, study questionnaires, and surveys, etc.

1. Park H, Islam MS, Grover MA, Klishko AN, Prilutsky BI, DeWeerth SP. A prototype of a neural, powered transtibial prosthesis for the cat: Benchtop characterization. Frontiers in Human Neuroscience. *Frontiers in Neuroscience* **12**: 471, 2018 (attached to this report).
2. Jarrell J, Farrell BJ, Kistenberg RS, Dalton JF, Pitkin M, Prilutsky BI. Kinetics of individual limbs during level and slope walking with a *unilateral transtibial bone-anchored prosthesis in the cat. Journal of Biomechanics,* ***76****: 74-83, 2018* (attached to this report).

Journal of Biomechanics xxx (2018) xxx–xxx

Contents lists available at ScienceDirect

Journal of Biomechanics

journal homepage: www.elsevier.com/locate/jbiomech
www.JBiomech.com

Kinetics of individual limbs during level and slope walking with a unilateral transtibial bone-anchored prosthesis in the cat

Joshua R. Jarrell [a], Brad J. Farrell [b], Robert S. Kistenberg [a], John F. Dalton IV [c], Mark Pitkin [d,e], Boris I. Prilutsky [a,*]

[a] School of Biological Sciences, Georgia Institute of Technology, Atlanta, GA, USA
[b] Department of Physical Therapy, Georgia State University, Atlanta, GA, USA
[c] Georgia Hand, Shoulder & Elbow, Atlanta, GA, USA
[d] Tufts University School of Medicine, Boston, MA, USA
[e] Poly-Orth International, Sharon, MA, USA

ARTICLE INFO

Article history:
Accepted 13 May 2018
Available online xxxx

Keywords:
Porous titanium implant
Bone-anchored prostheses
Prosthetic quadrupedal walking
Cat

ABSTRACT

Ongoing animal preclinical studies on transcutaneous bone-anchored prostheses have aimed to improve biomechanics of prosthetic locomotion in people with limb loss. It is much less common to translate successful developments in human biomechanics and prosthetic research to veterinary medicine to treat animals with limb loss. Current standard of care in veterinary medicine is amputation of the whole limb if a distal segment cannot be salvaged. Bone-anchored transcutaneous prostheses, developed for people with limb loss, could be beneficial for veterinary practice. The aim of this study was to examined if and how cats utilize the limb with a bone-anchored passive transtibial prosthesis during level and slope walking. Four cats were implanted with a porous titanium implant into the right distal tibia. Ground reaction forces and full-body kinematics were recorded during level and slope (±50%) walking before and 4–6 months after implantation and prosthesis attachment. The duty factor of the prosthetic limb exceeded zero in all cats and slope conditions ($p < 0.05$) and was in the range of 45.0–60.6%. Thus, cats utilized the prosthetic leg for locomotion instead of walking on three legs. Ground reaction forces, power and work of the prosthetic limb were reduced compared to intact locomotion, whereas those of the contralateral hind- and forelimbs increased ($p < 0.05$). This asymmetry was likely caused by insufficient energy generation for propulsion by the prosthetic leg, as no signs of pain or discomfort were observed in the animals. We concluded that cats could utilize a unilateral bone-anchored transtibial prosthesis for quadrupedal level and slope locomotion.

1. Introduction

It is a common practice to use animal models to investigate biomechanical function, safety and efficacy of orthopedic and prosthetic implants, procedures and technologies for translation to human clinical practice. For example, ongoing animal studies on transcutaneous porous titanium bone implants (Farrell et al., 2014a,b; Fitzpatrick et al., 2011; Pitkin et al., 2009; Shelton et al., 2011) have aimed to reduce skin infection in individuals with bone-anchored lower limb prostheses (Branemark et al., 2014; Drygas et al., 2008; Tillander et al., 2010; Tsikandylakis et al., 2014), and ultimately to improve biomechanics of prosthetic locomotion. It is much less common, however, to translate successful developments in human biomechanics, orthopedic and prosthetic research to veterinary medicine to treat animals with limb loss. According to Mich (2014), the current dogma in veterinary medicine of quadrupedal pets (dogs and cats) is: "animals do great on 3 legs". As a result, standard of care in veterinary medicine is amputation of the whole limb if a distal segment (e.g., foot) cannot be salvaged. This, in turn, leads to animal limited mobility, weight gain, break-down of a sound limb, chronic neck and back pain, and premature euthanasia (Mich, 2014; Mich et al., 2013). The method of direct attachment of a prosthesis to the residual limb, developed for people with limb loss, could be beneficial for veterinary practice.

Direct attachment of limb prosthesis to the residual bone using a transcutaneous solid titanium implant inside the medullary cavity has been used in individuals with limb loss since the 1990s

* Corresponding author at: School of Biological Sciences, Georgia Institute of Technology, 555 14th Street NW, Atlanta, GA 30332-0356, USA.
E-mail address: boris.prilutsky@ap.gatech.edu (B.I. Prilutsky).

https://doi.org/10.1016/j.jbiomech.2018.05.021
0021-9290/

(Branemark et al., 2001; Hagberg and Branemark, 2009; Jonsson et al., 2011; Van de Meent et al., 2013). Several advantages of bone-anchored limb prostheses over conventional socket-attached prostheses have been reported. Bone-anchored prostheses improve load transmission, eliminate skin problems caused by skin friction inside the socket (irritation, blisters, edema and dermatitis) (Hagberg and Branemark, 2009; Jonsson et al., 2011; Juhnke et al., 2015), and increase range of motion (Hagberg et al., 2005; Tranberg et al., 2011). Bone-anchored prostheses improve comfort and confidence of the users (Hagberg et al., 2008; Lundberg et al., 2011; Witso et al., 2006) and permit easier donning and doffing of the prosthesis (Jonsson et al., 2011). In addition, bone-anchored prostheses improve perception of prosthesis loading, defined as osseoperception (Haggstrom et al., 2013a; Jacobs et al., 2000; Lundborg et al., 2006), lead to fewer clinical visits to the prosthetist (Haggstrom et al., 2013b), and result in improvement of walking mechanics (Frossard et al., 2013; Hagberg et al., 2005; Tranberg et al., 2011).

All these advantages of bone-anchored prostheses would be beneficial to quadrupedal animals with limb loss if animals choose to utilize a prosthesis on one leg over locomoting on three sound legs, as currently assumed in veterinary medicine (Mich, 2014). Although few case report studies have suggested that quadrupedal animals might utilize a unilateral distal bone-anchored prosthesis for walking (Farrell et al., 2014a; Fitzpatrick et al., 2011), no studies have been published that rigorously document whether quadrupedal animals systematically utilize unilateral transtibial prostheses during locomotion and how prosthetic locomotion is performed. The use of the prosthetic limb during quadrupedal locomotion might depend on which limb is missing (forelimb versus hindlimb) and on loading demands on the prosthetic limb. For example, during downslope walking at grade 50%, peak loading on the hindlimbs is reduced by ~25% compared to 50%-upslope walking (Gregor et al., 2006; Prilutsky et al., 2011). Reduced loading on the prosthetic limb could prompt the animal not to utilize the prosthesis at all and to locomote on three legs instead.

Therefore, the aim of this study was to examined if and how cats utilize the limb with a bone-anchored passive transtibial prosthesis during downslope, level and upslope walking. We judged whether the animal used the prosthetic limb for locomotion based on the duty factor (the ratio of the stance phase duration over the cycle duration). We hypothesized that the duty factor will not be zero, i.e. the stance phase of the prosthetic limb would be present. If the first hypothesis was confirmed, one would expect a reduced loading of the prosthetic leg during locomotion as observed in people walking with a unilateral passive transtibial prosthesis (Barr et al., 1992; Fey et al., 2011; Segal et al., 2006). Therefore, if the animals would utilize quadrupedal gait with the prosthesis, we would test a second hypothesis that the ground reaction forces and work done by the prosthetic limb would be reduced compared to those of the sound limbs.

2. Methods

Full descriptions of the surgical and rehabilitative procedures, prosthesis and implant design, and data acquisition have been published previously (Farrell et al., 2014a) and only briefly described here. All experimental procedures were in agreement with the US Public Health Service Policy on Humane Care and Use of Laboratory Animals and were approved by the Institutional Animal Care and Use Committees at both Georgia Institute of Technology and St. Joseph's Translational Research Institute (now known as T3 Labs).

The subjects were four adult purpose-bred cats (baseline mass range 3.0–3.2 kg, Table 1) from our ongoing translational study on integration of the titanium porous Skin- and Bone-Integrated Pylon (SBIP; Poly-Orth International; Sharon MA, USA) with the residual limb (Farrell et al., 2014a; Jarrell et al., 2016, 2017). The cats were trained (~2 h a day, 5 days a week for 3–4 weeks) to walk along an enclosed walkway with 3 embedded force platforms (Bertec Corporation, Columbus OH, USA). The walkway was set at three slopes: 0% (level), 50% (upslope), and -50% (downslope). At the end of the training period, full-body kinematics and ground reaction forces were recorded by a 6-camera motion capture system (Vicon, UK) and the force platforms during level and sloped walking.

Prior to implantation, sagittal and frontal plane X-ray images of the right tibia of each cat were taken to evaluate the size and shape of the medullary canal. Porous titanium SBIP implants were obtained from Poly-Orth International (Sharon, MA, USA). Implants had a tapered design similar to the tibial marrow cavity, which was reamed to a press fit. The distinction of the SBIP from existing systems for direct skeletal attachment of limb prostheses (Pitkin, 2013) is its total permeability achieved in a structure consisting of porous cladding and perforated inserts (Pitkin et al., 2012). The SBIP material specification has a uniquely selected combination of four critical parameters: particle size, pore size, porosity and volume fraction (Pitkin and Raykhtsaum, 2012). This allows for deep ingrowth of the hosting tissues of bone and skin in combination with implant durability and resistance to fatigue (Farrell et al., 2014a,b; Pitkin et al., 2009).

After implantation surgery, performed on the right hindlimb in each cat under sterile conditions with isoflurane anesthesia, the residual right hindlimb with implant (prosthetic limb) was casted for 10 weeks to prevent premature loading (Farrell et al., 2014a). During weeks 6 through 10 after implantation, the distal end of the protruding implant was loaded for 15 min 3 times a week using a hand-held digital dynamometer (Accu-Force Cadet, Ametek, Largo, FL, USA) with gradually increased forces in each week from ~4% to 45% of body weight with a step of 10% (Farrell et al., 2014a). During this procedure, the animal, laying on the left side, was fed and petted by a researcher, while another one gently applied the specified load to the implant. This procedure aimed to strengthen bone-implant integration and was similar in terms of the loading initiation time, duration and magnitude to those used in individuals with press-fitted titanium implants for bone-anchored transfemoral prostheses (Aschoff et al., 2010; Juhnke et al., 2015). Starting with week 11, the cast was removed and a prosthesis was attached to the SBIP.

The cat was trained to stand and walk on the prosthesis with food reward for 4–6 weeks (the same training protocol as before surgery). After the animal started walking on the J-shaped transtibial prosthesis, level and slope locomotion was recorded several days a week for at least 4 weeks.

Data for slope walking in the first studied cat (cat QMV5, Table 1) were not collected due to uncertainty about the ability of cats with a transtibial passive prosthesis to walk on slopes. Data of cat 11NLS4 for level intact walking were of poor quality and could not be analyzed. Since there were no intact control data for this cat during level walking, prosthetic level walking was not collected. Number of analyzed cycles per limb in each slope condition pre and post implantation are summarized in Table 2.

After locomotion data were collected, the animal was euthanized using deep anesthesia (an overdose of sodium pentobarbital, 120–180 mg/kg, IV) and the residual shank with the implant was harvested for histological analysis as described in (Farrell et al., 2014a).

A full-body inverse dynamics analysis in the sagittal plane was performed to determine the resultant moments at hindlimb and forelimb joints, and subsequently their negative and positive power and work (Prilutsky and Klishko, 2011; Prilutsky et al.,

Please cite this article in press as: Jarrell, J.R., et al. Kinetics of individual limbs during level and slope walking with a unilateral transtibial bone-anchored prosthesis in the cat. J. Biomech. (2018), https://doi.org/10.1016/j.jbiomech.2018.05.021

Table 1
Animal characteristics.

Cat characteristics	QM04	09NHT4	11NLS4	QMV5	Mean ± SD
Baseline mass, kg	3.2	3.2	3.2	3.0	3.15 ± 0.10
Terminal mass, kg	4.0	3.4	2.8	4.0	3.55 ± 0.57
Estimated mass of the foot and distal third tibia, g	54.1	52.5	49.5	51.2	51.8 ± 2.0
Estimated moment of inertia of the foot and distal third tibia, g cm^2	290	326	279	281	294 ± 22
Prosthesis mass, g	15.5	15.5	18.4	18.4	17.0 ± 1.8
Prosthesis moment of inertia with respect to frontal axis through prosthesis center of mass, g cm^2	172	172	157	157	164.5 ± 8.7
Baseline walking speed, m/s					
Level	0.67 ± 0.06	0.46 ± 0.02	–	0.54 ± 0.04	0.56 ± 0.10
Downslope	0.75 ± 0.14	0.55 ± 0.06	0.58 ± 0.10	–	0.61 ± 0.13
Upslope	0.56 ± 0.21	0.40 ± 0.07	0.71 ± 0.20	–	0.55 ± 0.20
Terminal walking speed, m/s					
Level	0.50 ± 0.07	0.39 ± 0.03	–	0.40 ± 0.03	0.44 ± 0.07*
Downslope	0.61 ± 0.07	0.32 ± 0.08	0.59 ± 0.07	–	0.47 ± 0.16*
Upslope	0.54 ± 0.14	0.41 ± 0.09	0.42 ± 0.04	–	0.47 ± 0.12*

Notes: The term 'Terminal' designates measurements taken several days before euthanasia. Asterisks '*' indicate significant difference ($p < 0.05$) between intact and prosthetic walking.

Table 2
Number of cycles used for analysis of each limb.

Limb Walking conditions	Prosthetic right hindlimb	Contralateral hindlimb	Ipsilateral forelimb	Contralateral forelimb
Pre implantation walking				
Level	14	12	14	13
Downslope	12	17	14	19
Upslope	17	17	13	13
Post implantation walking				
Level	15	13	21	15
Downslope	14	11	15	13
Upslope	14	13	10	12

2005) before implantation and during prosthetic walking. Inertial properties of the prosthesis were determined using measurements of prosthesis weight, as well as suspension and geometric methods (Farrell et al., 2014a). Mass of the prosthesis was smaller than the estimated mass of the foot and distal third of the tibia that the prosthesis substituted (Table 1).

The limb duty factor and the mean walking speed in the cycle were calculated for each limb and cycle and averaged across cycles for each animal and slope condition and across animals. The time-dependent kinetic variables (tangential and normal ground reaction forces, GRFx and GRFz, respectively, and joint powers) were time-normalized to the duration of the stride of the corresponding limb. Powers were computed for individual joints of each limb: metatarsophalangeal, ankle, knee, and hip joints for hindlimbs and metacarpophalangeal, wrist, elbow and shoulder joints for forelimbs. Each time-normalized variable was averaged at each percent of the cycle across cycles of the corresponding limb for each cat and across cats. Total negative and positive work of each limb was obtained from the total limb power computed as the sum of powers in individual joints. All kinetic variables were also amplitude-normalized to subject's body mass.

IBM SPSS Statistics software, v24 (IBM SPSS, Chicago IL, USA) was used to test hypotheses of the study. In these tests, cats served as their own controls. The one-sample T-test (or the one-sample Wilcoxon signed rank test when the variable was not normally distributed) was used to test the hypothesis that the duty factor of the prosthetic limb differed from zero, i.e. the animals utilized quadrupedal locomotion with the prosthesis. These tests were performed on individual animals and across all animals. To test if the duty factor, peak GRF, and work of the prosthetic limb pre and post implantation differed from those of the sound limbs, we used a mixed linear model analysis (Brown and Prescott, 2006; West et al., 2015). This analysis takes the advantage of a within-subject design and using all individual trials of each subject. That increases statistical power of the analysis and makes it suitable for analyzing small-sample data sets. Given a small number of subjects, the mixed linear model analysis was first performed on each cat. In this analysis, the fixed factors were walking condition (pre implantation, post implantation), limb (prosthetic right hindlimb, PH; ipsilateral forelimb, IF; contralateral hindlimb, CH; contralateral forelimb, CF), and walking slope (level, downslope, upslope). The dependent variables were the duty factor, peak of GRFz, and total positive work of the limb. The post hoc comparisons with Bonferroni adjustments were performed when a fixed factor was found to be significant. In addition, the same analysis was performed across all cats; to do that a random factor Cat was added. To account for a possible influence of the walking speed on kinetic variables (Lelas et al., 2003), the cycle time of the corresponding limb was used as a covariate in all mixed linear model analyses. The cycle time was considered a better covariate than walking speed due to interlimb variability of cycle time.

To compare patterns of kinetic variables within the walking cycle between pre and post implantation walking, the wavelet-based functional ANOVA (wfANOVA) analysis was used (McKay et al., 2013; Potocanac et al., 2016). This method reveals differences in the shape and magnitude of time-dependent variables with both high temporal resolution and high statistical power (McKay et al., 2013). Significance level in all statistical tests was set at 0.05.

3. Results

No signs of discomfort or pain were observed in the animals during the post-surgical pylon loading in weeks 6 through 10 (the absence of limb withdrawal) or during prosthetic use. Behavioral observations of the prosthesis use indicated that the cats engaged the prosthesis for standing, walking, and, occasionally, jumping.

3.1. Duty factor

Since the independent fixed factor of slope did not significantly affect the duty factor ($F_{2,268} = 1.913$, $p = 0.150$), statistical tests on the duty factor were performed across the three slope conditions. The duty factor of the prosthetic hindlimb (PH) during walking was significantly different from zero for each of 4 animals (QM04: 0.62 ± 0.09, $p = 0.001$; 09NHT4: 0.62 ± 0.09, $p < 0.001$; 11NLS4: 0.44 ± 0.18, $p < 0.003$; QMV5: 0.56 ± 0.02, $p < 0.001$), see Fig. 1A. The duty factor for the prosthetic hindlimb was shorter in post implantation walking than in intact pre implantation walking in 3 out of 4 cats ($F_{1,268} = 14.6–85.3$, $p \leq 0.001$; Fig. 1A). For the contralateral hindlimb (CH) and forelimb (CF), the duty factor was greater in post than in pre implantation walking in each animal ($F_{1,268} = 4.8–84.0$, $p \leq 0.001–0.029$; Fig. 1A). The duty factor of the prosthetic hindlimb analyzed across all slopes and cats, was smaller in post implantation than in intact pre implantation walking ($F_{1,268} = 84.4$, $p < 0.001$), whereas the duty factor of the remaining 3 limbs was higher during post compared to pre walking ($F_{1,268} = 4.2–180.1$, $p \leq 0.001–0.041$; Fig. 1B).

3.2. Ground reaction forces

During the stance phase of post implantation walking, the prosthetic hindlimb of each cat exerted substantial peaks of the normal ground reaction force in all slope conditions (GRFz, ~2–4 N/kg) that, however, were lower than the GRFz peak values prior to surgery in 3 out of 4 cats (~4–5 N/kg, $F_{1,268} = 17.7–207.4$, $p < 0.001$; Fig. 1C, 2). The contralateral hind- and forelimb exerted larger peaks of GRFz during post than pre implantation walking in all cats, while the ipsilateral forelimb demonstrated higher peak forces in 3 out of 4 cats ($F_{1,268} = 4.2–25.1$, $p < 0.041$; Fig. 1C, 2).

GRFz values of the prosthetic hindlimb post implantation were lower than those of the same limb before surgery in early and mid-stance of downslope walking, in early and late stance of level walking, and in the entire stance of upslope walking (wfANOVA, $p < 0.05$; Fig. 2, shaded areas). GRFz of the contralateral hindlimb and forelimb increased in late stance of post implantation walking in all slope conditions, as well as in early stance of downslope and level walking (wfANOVA, $p < 0.05$; Fig. 2). Peaks of GRFz of the prosthetic hindlimb post implantation decreased by 30%, 45%, and 46% during level, downslope, and upslope walking, respectively ($F_{1,312} = 27.1–90.5$, $p < 0.001$). The GRFz peak of contralateral hindlimb and forelimb increased during post implantation walking in all slope conditions in the range of 16%-60% ($F_{1,312} = 11.1–68.0$, $p \leq 0.001$). A small significant increase in GRFz peak of ipsilateral forelimb occurred during post implantation level walking (10%, $F_{1,313} = 4.5$, $p = 0.035$).

GRFx values of the prosthetic hindlimb were lower after implantation throughout most of the stance phase duration in all slope walking conditions (as revealed by the wfANOVA, $p < 0.05$, shaded areas in Fig. 3). GRFx values in the contralateral hindlimb and forelimb were higher in substantial portions of stance during post implantation walking (wfANOVA, $p < 0.05$). Compared to pre implantation walking, ipsilateral forelimb GRFx during prosthetic walking was slightly but significantly higher in the terminal period of stance in upslope condition, and it was lower in the initial and terminal periods of stance in level condition. No difference in ipsilateral forelimb GRFx between post and pre implantation walking was observed in downslope condition ($p > 0.05$; Fig. 3). GRFx peaks in the prosthetic hindlimb post implantation were lower than during pre implantation walking in level (acceleratory force by 59%: $F_{1,316} = 25.7$, $p < 0.001$; braking force by 52%: $F_{1,316} = 14.9$, $p < 0.001$), downslope (braking force by 66%: $F_{1,316} = 133.3$, $p < 0.001$), and upslope conditions (acceleratory force by 54%; $F_{1,316} = 181.8$, $p < 0.001$). GRFx peaks of the contralateral hindlimb and forelimb were higher in downslope (braking force by 22–33%: $F_{1,316} = 31.2–47.7$, $p < 0.001$) and upslope (acceleratory force by 21–85%: $F_{1,316} = 29.4–143.8$, $p < 0.001$) conditions of prosthetic walking (Fig. 3).

3.3. Total limb power and work

Little power and work was produced by the prosthetic hindlimb post implantation in all slope conditions (Figs. 4 and 5). During pre implantation walking, the same hindlimb produced negative power (absorbed mechanical energy) in the stance phase of downslope walking and first third of stance of level walking; positive power (energy generation) was produced in last two thirds of the stance phase of level walking and during the entire stance of upslope walking. In three out of four cats, positive work done by the prosthetic limb post implantation was lower than that of the same limb before surgery ($F_{1,268} = 12.6–78.0$, $p < 0.001$; Fig. 1D). The contralateral hindlimb produced higher negative and positive power and work during post implantation walking in all slope conditions (wfANOVA, $p = 0.05$; Figs. 4 and 5). In three of four cats, positive work of the contralateral hindlimb was higher during post implantation than pre implantation walking ($F_{1,268} = 4.9–84.6$, $p \leq 0.001–0.027$; Fig. 1D).

Forelimbs produced primarily negative power and did negative work during pre implantation walking in downslope and level conditions. During post implantation level walking, both contralateral and ipsilateral forelimbs generated mostly positive power and work. During post implantation downslope walking, the contralateral forelimb produced more negative power in the end of stance (wfANOVA, $p = 0.05$; Fig. 4). There was less difference in power generation and work done between post and pre implantation walking in the ipsilateral and contralateral forelimbs in individual cats and across all cats (Figs. 1D, 4 and 5).

4. Discussion

The results of the study supported the hypothesis that cats with a SBIP-attached unilateral transtibial prosthesis would use it for support during quadrupedal locomotion – the duty factor of the prosthetic limb exceeded zero and was in the range of 45.0–60.6% for all cats. Additionally, the prosthetic limb generated substantial normal GRF during level and slope walking post implantation. The second hypothesis that the GRF and work values produced by the prosthetic limb would be lower compared to the sound limbs post implantation was also supported. Thus, the current standard of care in veterinary medicine, i.e. amputation of the whole limb if a distal limb segment cannot be salvaged, should be reexamined. In our study, all four cats utilized the unilateral transtibial prosthesis for walking rather than ambulating on three legs. Although quadrupedal prosthetic walking is still asymmetric (Figs. 1–5) and this may lead to secondary conditions in the sound limbs, back and neck (Mich, 2014; Mich et al., 2013), the extent of this asymmetry is certainly smaller than that occurring during 3–legged locomotion (Fuchs et al., 2014).

It is important to note that the locomotor asymmetry documented in this study was not likely pain related. There were no observed clinical signs of discomfort or pain while loading the implant and prosthesis (no limb withdrawal) and no signs of infection on X-ray and histological images at the end of the study. A possible explanation for the reduced loading of the prosthetic limb

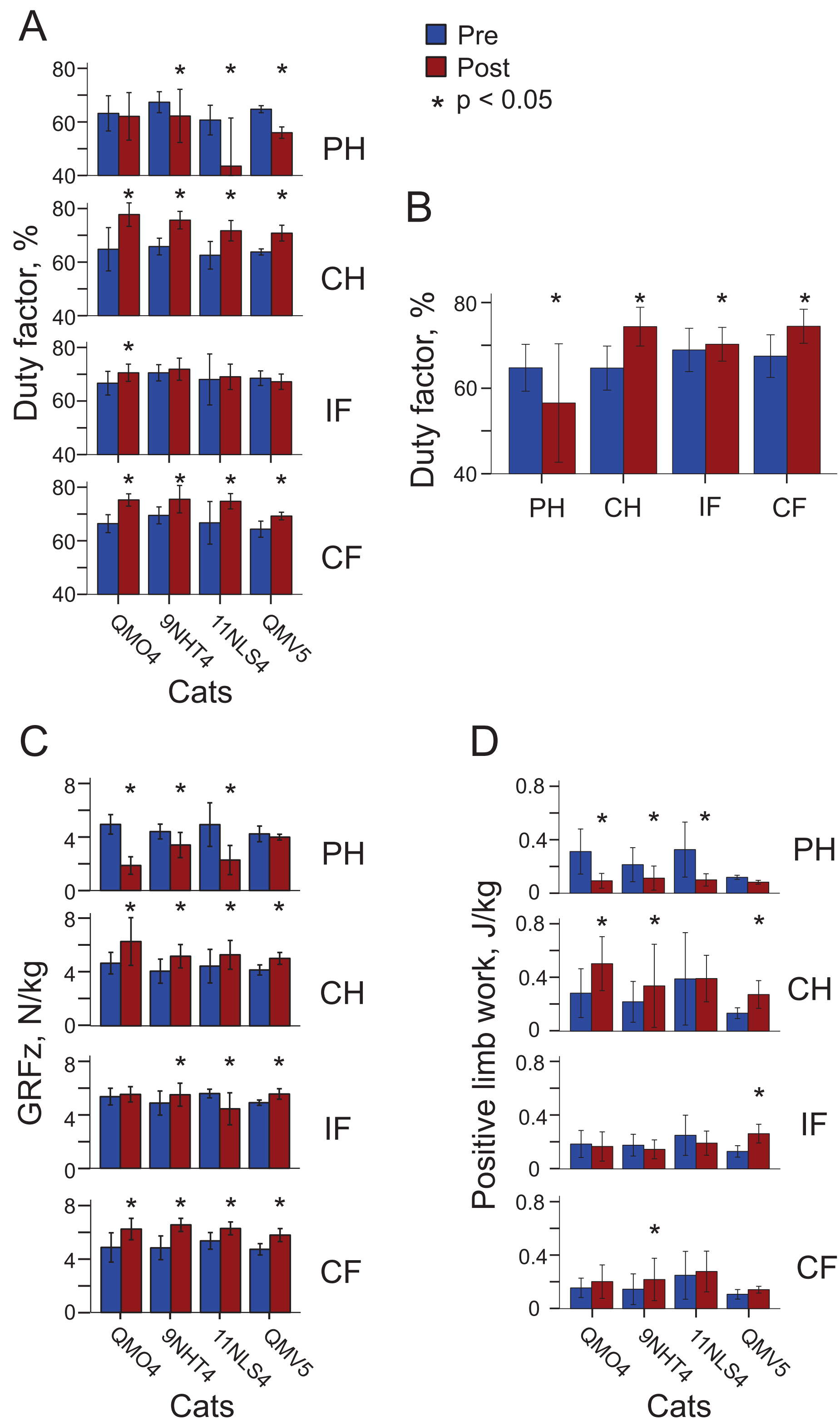

Fig. 1. Major kinematic and kinetic variables (mean ± SD) during pre (Pre) and post implantation (Post) walking in individual cats and limbs. Asterisks indicate significant differences ($p < 0.05$) between pre and post implantation conditions. PH, right hindlimb (prosthetic hindlimb in Post condition); CH, contralateral hindlimb; IF, ipsilateral forelimb; CF, contralateral forelimb. (A) Duty factor of individual cats averaged across all slope conditions and walking cycles. (B) Duty factor averaged across all cats, slope conditions and walking cycles. (C) Peaks of normal ground reaction force (GRFz) of individual cats averaged across all slope conditions and walking cycles. (D) Positive limb work of individual cats averaged across all slope conditions and walking cycles.

during walking might be the non-optimal length, alignment of the prosthesis and shape of the rocker bottom. These parameters were selected to approximately match the hindlimb length and orientation during the stance phase of normal cat walking (Farrell et al., 2014a). In addition, the decreased loading of the prosthetic limb may reflect the limited ability of the cat with the transtibial pros-

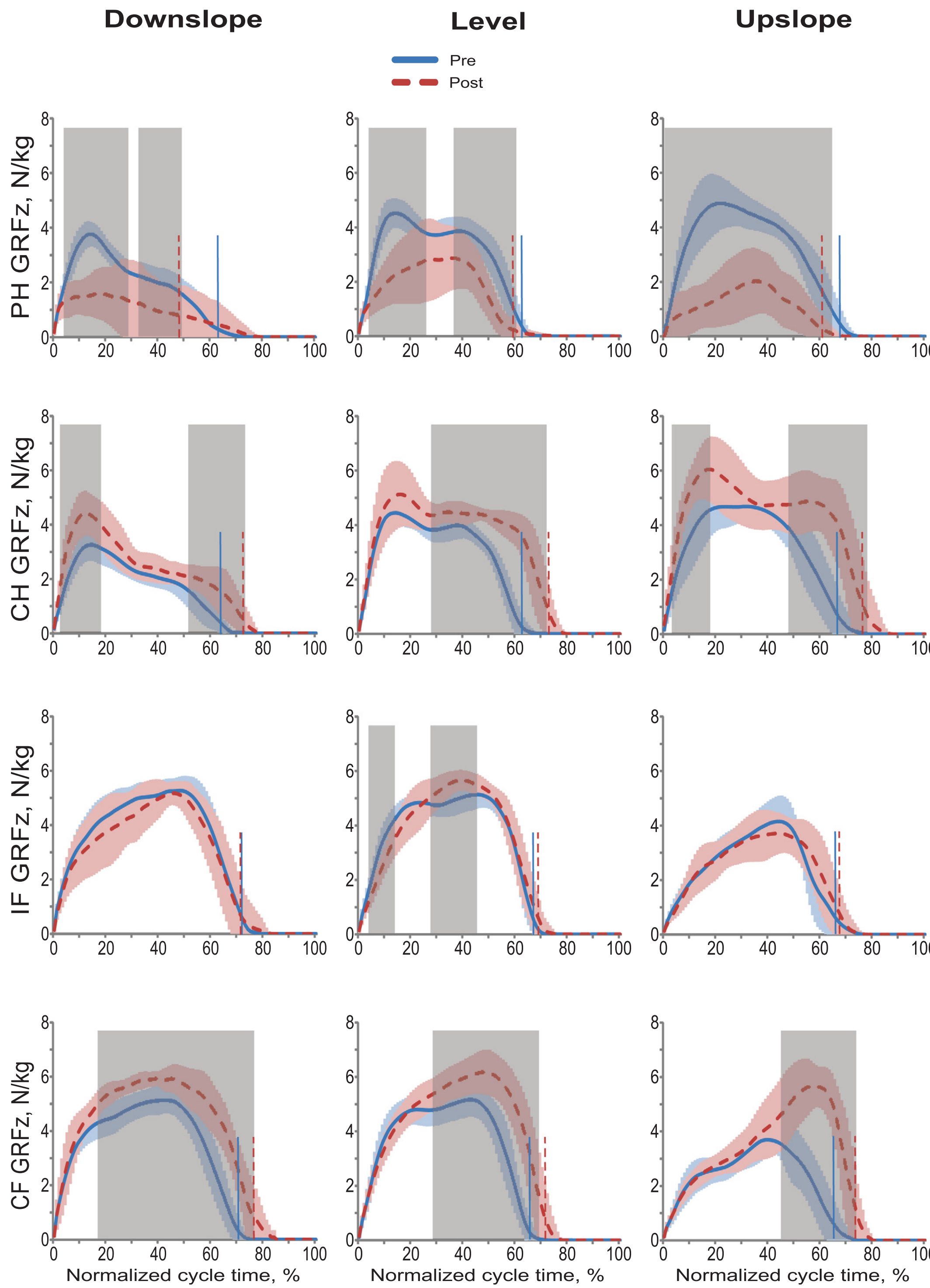

Fig. 2. Normalized normal ground reaction forces (GRFz) during the cycle of pre implantation (Pre) and post implantation (Post) walking in downslope (−50%), level (0%), and upslope (+50%) conditions. Mean (±SD) data of 4 animals. The vertical dashed and solid lines separate stance and swing phases for post and pre implantation walking, respectively. The shaded areas in each panel indicate significant difference ($p < 0.05$) between the pre and post implantation walking determined using wfANOVA analysis. PH, right hindlimb (prosthetic hindlimb in Post condition); CH, contralateral hindlimb; IF, ipsilateral forelimb; CF, contralateral forelimb.

thesis, which lacks an active ankle joint, to generate a sufficient amount of mechanical energy for propulsion. Note that the intact ankle in the cat does approximately 35% of total hindlimb positive work during level and upslope walking (McFadyen et al., 1999; Prilutsky and Klishko, 2011).

There was much greater symmetry between the prosthetic and sound limbs in the normal GRFz than in the tangential GRFx during post implantation walking (Figs. 1C, 2 and 3). For example, the normal GRFz applied to the prosthesis during walking exceeded 50% of the pre implantation walking values on average across all cats (Figs. 1C and 2). Peak GRFx values, however, were only between 34% (braking force in downslope walking) and 48% (braking force in level walking) of the pre implantation values (Fig. 3). One possible explanation for the

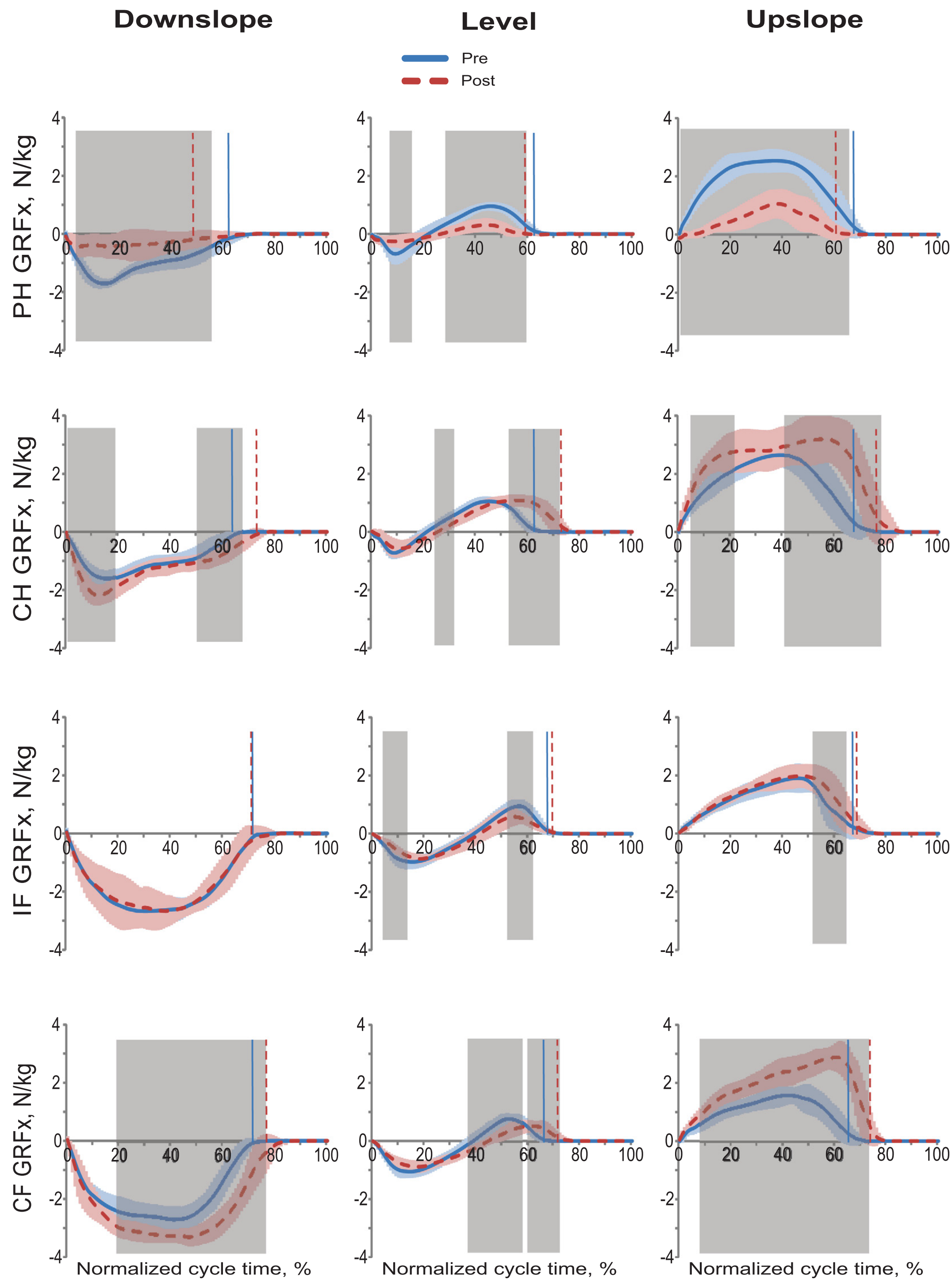

Fig. 3. Normalized tangential ground reaction forces (GRFx) during the cycle of pre implantation (Pre) and post implantation (Post) walking in downslope (−50%), level (0%), and upslope (+50%) conditions. Mean (±SD) data of 4 animals. The vertical dashed and solid lines separate stance and swing phases for post and pre implantation, respectively. The shaded areas in each panel indicate significant difference ($p < 0.05$) between the pre and post implantation walking determined using wfANOVA analysis. PH, right hindlimb (prosthetic hindlimb in Post condition); CH, contralateral hindlimb; IF, ipsilateral forelimb; CF, contralateral forelimb.

bigger decrease in GRFx compared to GRFz forces exerted by the prosthetic limb could be the reduced ability of the animal with a passive ankle to exert substantial tangential forces without slipping. The requirement to prevent slipping during stance might have forced the animal to reduce the ratio of the tangential to normal forces, known as the required coefficient of friction (Redfern et al., 2001).

The reduced loading of the prosthetic limb and greater loading of the sound contralateral limbs found in this study agreed well with previous results of dog locomotion with hindlimb lameness (Weishaupt et al., 2004) or hindlimb amputation (Fuchs et al., 2014), and of sheep prosthetic locomotion (Shelton et al., 2011). People with unilateral transtibial amputation also show reduced loading of the prosthetic leg and increased loading of the contralat-

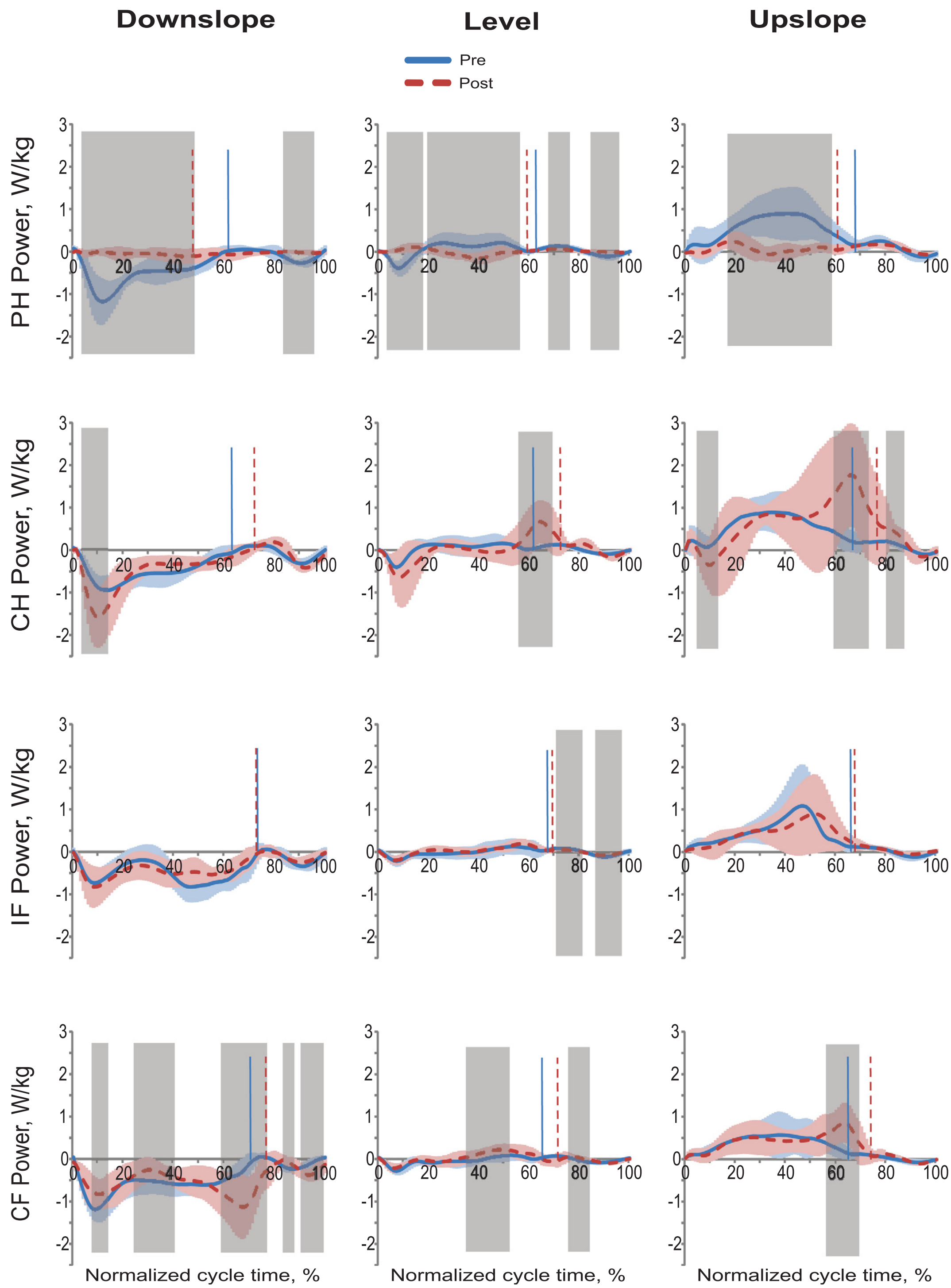

Fig. 4. Normalized power of each limb during the cycle of pre implantation (Pre) and post implantation (Post) walking in downslope (−50%), level (0%), and upslope (+50%) conditions. Mean (±SD) data of 4 animals. The vertical dashed and solid lines separate stance and swing phases for post and pre walking, respectively. The shaded areas in each panel indicate significant difference ($p < 0.05$) between the pre and post implantation walking determined using wfANOVA analysis. PH, right hindlimb (prosthetic hindlimb in Post condition); CH, contralateral hindlimb; IF, ipsilateral forelimb; CF, contralateral forelimb.

eral leg during prosthetic walking (Barr et al., 1992; Fey et al., 2011; Segal et al., 2006). As discussed above, these changes in prosthetic walking may be needed to compensate for the lack of energy generation by the passive prosthetic ankle joint. This suggestion is supported by the fact that during prosthetic walking in humans, power produced and work done at the contralateral leg increase (Beyaert et al., 2008). Cats apparently used a similar strategy to compensate for a reduced ability of the prosthetic limb to generate energy and do positive work (Figs. 1D, 5). Additional energy is generated by the contralateral hindlimb (Figs. 1D, 5) in late stance of level and upslope walking (Fig. 4). Note also that all cats increased the duty factor of the contralateral hind- and forelimb during prosthetic walking (Fig. 1A), which allowed relatively more time to generate mechanical energy.

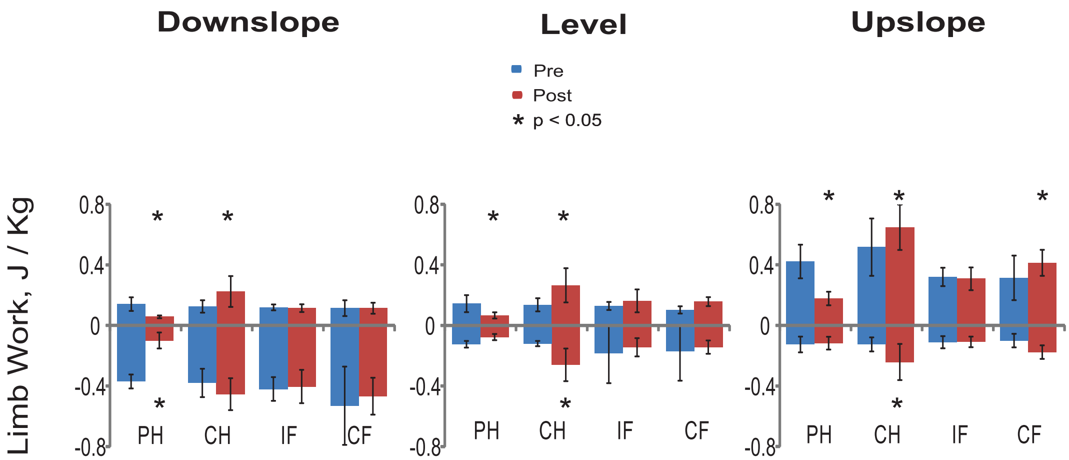

Fig. 5. Normalized negative and positive work done by four limbs during the cycle of pre (Pre) and post implantation (Post) walking in downslope (−50%), level (0%), and upslope (+50%) conditions. Mean (±SD) data of 4 animals. PH, right hindlimb (prosthetic hindlimb in Post condition); CH, contralateral hindlimb; IF, ipsilateral forelimb; CF, contralateral forelimb. Asterisks indicate significant differences (p<0.05) between pre and post implantation conditions.

Several limitations of this study should be mentioned. The limited number of subjects tested in this study was caused by the complexity of the procedures. The effects of this limitation was partially reduced by the statistical design we selected, i.e. the mixed linear model analysis (Brown and Prescott, 2006; West et al., 2015); see Methods for details. Although the small sample size limits our ability to generalize the results, the study nevertheless provides evidence that the titanium SBIP pylons with deep porosity can serve for anchoring transtibial limb prostheses and that the animals can adopt the prosthesis for walking. The observed large reduction in loading and utilization of the prosthetic limb during walking could be partially caused by a relatively short duration of the study. It is possible that if the study was longer, the loading and use of the prosthetic limb may have increased, and walking kinetics might have shifted more toward intact patterns as the cats became more familiar with the prostheses. There was uncertainty in the positioning of the markers on the prosthesis to specify the location of the metatarsophalangeal and ankle joints. This uncertainty should not have affected substantially the calculated power at the passive ankle.

In summary, the results of this study demonstrated that cats could utilize a unilateral bone-anchored transtibial prosthesis for quadrupedal level and slope locomotion. Although walking with the transtibial passive prosthesis was asymmetric, this asymmetry was lower than that reported for 3-legged locomotion. Thus, the current standard of care in veterinary medicine recommending amputation of the whole limb if a distal segment cannot be salvaged should be reexamined.

Acknowledgements

This study was supported in part by DOD grant W81XWH-16-1-0791, NIH grants T32HD055180, R44HD057492 and R44HD090768, and NSF grant 0946809. Any opinions, findings, and conclusions or recommendations expressed in this material are those of the authors and do not necessarily reflect the views of the National Institutes of Health, National Science Foundation or Department of Defense. We would like to thank Dr. Ashley Strong, Dr. Evan Goldberg and staff of the T3 Labs for their excellent veterinary assistance, Mr. Nihir Patel for his help with data analysis, and Dr. J. Lucas McKay for providing assistance and Matlab code for the wfANOVA analysis.

Conflict of interest statement

We certify that there is no conflict of interest with any financial organization regarding the material discussed in the manuscript.

References

Aschoff, H.H., Kennon, R.E., Keggi, J.M., Rubin, L.E., 2010. Transcutaneous, distal femoral, intramedullary attachment for above-the-knee prostheses: an endo-exo device. J. Bone Joint Surg.-Am. 92A, 180–186.
Barr, A.E., Siegel, K.L., Danoff, J.V., McGarvey 3rd, C.L., Tomasko, A., Sable, I., Stanhope, S.J., 1992. Biomechanical comparison of the energy-storing capabilities of SACH and Carbon Copy II prosthetic feet during the stance phase of gait in a person with below-knee amputation. Phys. Ther. 72, 344–354.
Beyaert, C., Grumillier, C., Martinet, N., Paysant, J., Andre, J.M., 2008. Compensatory mechanism involving the knee joint of the intact limb during gait in unilateral below-knee amputees. Gait Posture 28, 278–284.
Branemark, R., Berlin, O., Hagberg, K., Bergh, P., Gunterberg, B., Rydevik, B., 2014. A novel osseointegrated percutaneous prosthetic system for the treatment of patients with transfemoral amputation: A prospective study of 51 patients. The Bone Joint J. 96-B, 106–113.
Branemark, R., Branemark, P.I., Rydevik, B., Myers, R.R., 2001. Osseointegration in skeletal reconstruction and rehabilitation: A review. J. Rehabil. Res. Dev. 38, 175–181.
Brown, H., Prescott, R., 2006. Applied Mixed Models in Medicine. John Wiley & Sons Ltd, Chichester, West Sussex, England.
Drygas, K.A., Taylor, R., Sidebotham, C.G., Hugate, R.R., Mcalexander, H., 2008. Transcutaneous tibial implants: a surgical procedure for restoring ambulation after amputation of the distal aspect of the tibia in a dog. Vet. Surg. 37, 322–327.
Farrell, B.J., Prilutsky, B.I., Kistenberg, R.S., Dalton, J.F.t., Pitkin, M., 2014a. An animal model to evaluate skin-implant-bone integration and gait with a prosthesis directly attached to the residual limb. Clin. Biomech. (Bristol, Avon) 29, 336–349.
Farrell, B.J., Prilutsky, B.I., Ritter, J.M., Kelley, S., Popat, K., Pitkin, M., 2014b. Effects of pore size, implantation time, and nano-surface properties on rat skin ingrowth into percutaneous porous titanium implants. J. Biomed. Mater. Res. Part A 102, 1305–1315.
Fey, N.P., Klute, G.K., Neptune, R.R., 2011. The influence of energy storage and return foot stiffness on walking mechanics and muscle activity in below-knee amputees. Clin. Biomech. (Bristol, Avon) 26, 1025–1032.
Fitzpatrick, N., Smith, T.J., Pendegrass, C.J., Yeadon, R., Ring, M., Goodship, A.E., Blunn, G.W., 2011. Intraosseous transcutaneous amputation prosthesis (ITAP) for limb salvage in 4 dogs. Veterinary Surgery: VS 40, 909–925.
Frossard, L., Haggstrom, E., Hagberg, K., Branemark, R., 2013. Load applied on bone-anchored transfemoral prosthesis: Characterization of a prosthesis-A pilot study. J. Rehabil. Res. Dev. 50, 619–634.
Fuchs, A., Goldner, B., Nolte, I., Schilling, N., 2014. Ground reaction force adaptations to tripedal locomotion in dogs. Veterinary J. 201, 307–315.
Gregor, R.J., Smith, D.W., Prilutsky, B.I., 2006. Mechanics of slope walking in the cat: quantification of muscle load, length change, and ankle extensor EMG patterns. J. Neurophysiol. 95, 1397–1409.
Hagberg, K., Branemark, R., 2009. One hundred patients treated with osseointegrated transfemoral amputation prostheses–rehabilitation perspective. J. Rehabil. Res. Dev. 46, 331–344.

Hagberg, K., Branemark, R., Gunterberg, B., Rydevik, B., 2008. Osseointegrated trans-femoral amputation prostheses: prospective results of general and condition-specific quality of life in 18 patients at 2-year follow-up. Prosthet. Orthot. Int. 32, 29–41.
Hagberg, K., Häggström, E., Uden, M., Brånemark, R., 2005. Socket versus bone-anchored trans-femoral prostheses: Hip range of motion and sitting comfort. Prosthet. Orthot. Int. 29, 153–163.
Haggstrom, E., Hagberg, K., Rydevik, B., Branemark, R., 2013a. Vibrotactile evaluation: osseointegrated versus socket-suspended transfemoral prostheses. J. Rehabil. Res. Dev. 50, 1423–1434.
Haggstrom, E.E., Hansson, E., Hagberg, K., 2013b. Comparison of prosthetic costs and service between osseointegrated and conventional suspended transfemoral prostheses. Prosthet. Orthot. Int. 37, 152–160.
Jacobs, R., Branemark, R., Olmarker, K., Rydevik, B., Van Steenberghe, D., Branemark, P.I., 2000. Evaluation of the psychophysical detection threshold level for vibrotactile and pressure stimulation of prosthetic limbs using bone anchorage or soft tissue support. Prosthet. Orthot. Int. 24, 133–142.
Jarrell, J.R., Farrell, B.J., Kistenberg, R.S., Dalton, J.F., IV, Pitkin, M., Prilutsky, B.I., 2016. Cat level and slope walking with a transtibial osseointegrated prosthesis. In: First International Symposium on Innovations in Amputation Surgery and Prosthetic Technologies. Chicago, IL.
Jarrell, J.R., Farrell, B.J., Kistenberg, R.S., Dalton, J.F., IV, Pitkin, M., Prilutsky, B.I., 2017. Kinetics of quadrupedal level and slope walking in the cat with a unilateral transtibial prosthesis anchored to the bone via a porous titanium pylon. In: 7th International Conference Advances in Orthopaedic Osseointegration. Coronado, CA.
Jonsson, S., Caine-Winterberger, K., Branemark, R., 2011. Osseointegration amputation prostheses on the upper limbs: methods, prosthetics and rehabilitation. Prosthet. Orthot. Int. 35, 190–200.
Juhnke, D.L., Beck, J.P., Jeyapalina, S., Aschoff, H.H., 2015. Fifteen years of experience with Integral-Leg-Prosthesis: Cohort study of artificial limb attachment system. J. Rehabil. Res. Dev. 52, 407–420.
Lelas, J.L., Merriman, G.J., Riley, P.O., Kerrigan, D.C., 2003. Predicting peak kinematic and kinetic parameters from gait speed. Gait Posture 17, 106–112.
Lundberg, M., Hagberg, K., Bullington, J., 2011. My prosthesis as a part of me: a qualitative analysis of living with an osseointegrated prosthetic limb. Prosthet. Orthot. Int. 35, 207–214.
Lundborg, G., Waites, A., Bjoerkman, A., Rosen, B., Larsson, E.M., 2006. Functional magnetic resonance imaging shows cortical activation on sensory stimulation of an osseointegrated prosthetic thumb. Scand. J. Plast. Reconstr. Surg. Hand Surg. 40, 234–239.
McFadyen, B.J., Lavoie, S., Drew, T., 1999. Kinetic and energetic patterns for hindlimb obstacle avoidance during cat locomotion. Exp. Brain Res. 125, 502–510.
McKay, J.L., Welch, T.D., Vidakovic, B., Ting, L.H., 2013. Statistically significant contrasts between EMG waveforms revealed using wavelet-based functional ANOVA. J. Neurophysiol. 109, 591–602.
Mich, P.M., 2014. The emerging role of veterinary orthotics and prosthetics (V-OP) in small animal rehabilitation and pain management. Top Companion Anim. Med. 29, 10–19.
Mich, P.M., Fair, L., Borghese, I., 2013. Assistive devices, orthotic, prosthetics, bandaging. In: Van Dyke, J., Zink, M.C. (Eds.), Canine Sports Medicine and Rehabilitation. Wiley Blackwell, Ames, IA, pp. 201–208.
Pitkin, M., 2013. Design features of implants for direct skeletal attachment of limb prostheses. J. Biomed. Mater. Res. Part A 101, 3339–3348.
Pitkin, M., Pilling, J., Raykhtsaum, G., 2012. Mechanical properties of totally permeable titanium composite pylon for direct skeletal attachment. Journal of biomedical materials research. Part B, Appl. Biomater. 100, 993–999.
Pitkin, M., Raykhtsaum, G., 2012. Skin integrated device, US patent #8257435.
Pitkin, M., Raykhtsaum, G., Pilling, J., Shukeylo, Y., Moxson, V., Duz, V., Lewandowski, J., Connolly, R., Kistenberg, R.S., Dalton, J.F.I., Prilutsky, B., Jacobson, S., 2009. Mathematical modeling and mechanical and histopathological testing of porous prosthetic pylon for direct skeletal attachment. J. Rehabil. Res. Dev. 46, 315–330.
Potocanac, Z., Pijnappels, M., Verschueren, S., van Dieen, J., Duysens, J., 2016. Two-stage muscle activity responses in decisions about leg movement adjustments during trip recovery. J. Neurophysiol. 115, 143–156.
Prilutsky, B.I., Klishko, A.N., 2011. Control of locomotion: Lessons from whole-body biomechanical analysis. In: Danion, F., Latash, M.L. (Eds.), Motor Control: Theories Experiments and Applications. Oxford University Press, Oxford, pp. 197–218.
Prilutsky, B.I., Maas, H., Bulgakova, M., Hodson-Tole, E.F., Gregor, R.J., 2011. Short-term motor compensations to denervation of feline soleus and lateral gastrocnemius result in preservation of ankle mechanical output during locomotion. Cells Tissues Organs 193, 310–324.
Prilutsky, B.I., Sirota, M.G., Gregor, R.J., Beloozerova, I.N., 2005. Quantification of motor cortex activity and full-body biomechanics during unconstrained locomotion. J. Neurophysiol. 94, 2959–2969.
Redfern, M.S., Cham, R., Gielo-Perczak, K., Gronqvist, R., Hirvonen, M., Lanshammar, H., Marpet, M., Pai, C.Y., Powers, C., 2001. Biomechanics of slips. Ergonomics 44, 1138–1166.
Segal, A.D., Orendurff, M.S., Klute, G.K., McDowell, M.L., Pecoraro, J.A., Shofer, J., Czerniecki, J.M., 2006. Kinematic and kinetic comparisons of transfemoral amputee gait using C-Leg and Mauch SNS prosthetic knees. J. Rehabil. Res. Dev. 43, 857–870.
Shelton, T.J., Beck, J.P., Bloebaum, R.D., Bachus, K.N., 2011. Percutaneous osseointegrated prostheses for amputees: Limb compensation in a 12-month ovine model. J. Biomech. 44, 2601–2606.
Tillander, J., Hagberg, K., Hagberg, L., Branemark, R., 2010. Osseointegrated titanium implants for limb prostheses attachments: infectious complications. Clin. Orthopaed. Related Res. 468, 2781–2788.
Tranberg, R., Zugner, R., Karrholm, J., 2011. Improvements in hip- and pelvic motion for patients with osseointegrated trans-femoral prostheses. Gait Posture 33, 165–168.
Tsikandylakis, G., Berlin, O., Branemark, R., 2014. Implant survival, adverse events, and bone remodeling of osseointegrated percutaneous implants for transhumeral amputees. Clin. Orthopaed. Related Res. 472, 2947–2956.
Van de Meent, H., Hopman, M.T., Frolke, J.P., 2013. Walking ability and quality of life in subjects with transfemoral amputation: a comparison of osseointegration with socket prostheses. Arch Phys. Med. Rehabil. 94, 2174–2178.
Weishaupt, M.A., Wiestner, T., Hogg, H.P., Jordan, P., Auer, J.A., 2004. Compensatory load redistribution of horses with induced weightbearing hindlimb lameness trotting on a treadmill. Equine Vet. J. 36, 727–733.
West, B.T., Welch, K.B., Gatecki, A.T., 2015. Linear Mixed Models. A Practical Guide using Statistical Software. CRC Press, Boca Raton, FL.
Witso, E., Kristensen, T., Benum, P., Sivertsen, S., Persen, L., Funderud, A., Magne, T., Aursand, H.P., Aamodt, A., 2006. Improved comfort and function of arm prosthesis after implantation of a Humerus-T-Prosthesis in trans-humeral amputees. Prosthet. Orthot. Int. 30, 270–278.

frontiers in Neuroscience

ORIGINAL RESEARCH
published: 13 July 2018
doi: 10.3389/fnins.2018.00471

Check for updates

A Prototype of a Neural, Powered, Transtibial Prosthesis for the Cat: Benchtop Characterization

Hangue Park[1,2†], Muhammad S. Islam[3], Martha A. Grover[4], Alexander N. Klishko[2], Boris I. Prilutsky[2] and Stephen P. DeWeerth[1,5]*

[1] School of Electrical and Computer Engineering, Georgia Institute of Technology, Atlanta, GA, United States, [2] Biomechanics and Motor Control Laboratory, School of Biological Sciences, Georgia Institute of Technology, Atlanta, GA, United States, [3] Wallace H. Coulter Department of Biomedical Engineering, Georgia Institute of Technology, Atlanta, GA, United States, [4] School of Chemical & Biomolecular Engineering, Georgia Institute of Technology, Atlanta, GA, United States, [5] P.C. Rossin College of Engineering and Applied Science, Lehigh University, Bethlehem, PA, United States

OPEN ACCESS

Edited by:
Daniel P. Ferris,
University of Florida, United States

Reviewed by:
Elliott J. Rouse,
University of Michigan, United States
Corey Pew,
University of Texas at Austin,
United States

***Correspondence:**
Boris I. Prilutsky
boris.prilutsky@ap.gatech.edu

†Present address:
Hangue Park,
Department of Electrical and Computer Engineering, Texas A&M University, College Station, TX, United States

Specialty section:
This article was submitted to Neuroprosthetics, a section of the journal Frontiers in Neuroscience

Received: 30 December 2017
Accepted: 21 June 2018
Published: 13 July 2018

Citation:
Park H, Islam MS, Grover MA, Klishko AN, Prilutsky BI and DeWeerth SP (2018) A Prototype of a Neural, Powered, Transtibial Prosthesis for the Cat: Benchtop Characterization. Front. Neurosci. 12:471. doi: 10.3389/fnins.2018.00471

We developed a prototype of a neural, powered, transtibial prosthesis for the use in a feline model of prosthetic gait. The prosthesis was designed for attachment to a percutaneous porous titanium implant integrated with bone, skin, and residual nerves and muscles. In the benchtop testing, the prosthesis was fixed in a testing rig and subjected to rhythmic vertical displacements and interactions with the ground at a cadence corresponding to cat walking. Several prosthesis functions were evaluated. They included sensing ground contact, control of transitions between the finite states of prosthesis loading, and a closed-loop modulation of the linear actuator gain in each loading cycle. The prosthetic design parameters (prosthesis length = 55 mm, mass = 63 g, peak extension moment = 1 Nm) corresponded closely to those of the cat foot-ankle with distal shank and the peak ankle extension moment during level walking. The linear actuator operated the prosthetic ankle joint using inputs emulating myoelectric activity of residual muscles. The linear actuator gain was modulated in each cycle to minimize the difference between the peak of ground reaction forces (GRF) recorded by a ground force sensor and a target force value. The benchtop test results demonstrated a close agreement between the GRF peaks and patterns produced by the prosthesis and by cats during level walking.

Keywords: bone-anchored transtibial prosthesis, sensing and powered prosthesis, closed-loop control, cat, ground reaction force

INTRODUCTION

Individuals with lower limb loss wearing a unilateral passive prosthesis frequently show asymmetric walking, which can lead to undesirable compensations and subsequent degenerative musculoskeletal conditions (Burke et al., 1978; Jaegers et al., 1995; Struyf et al., 2009). Among the variety of underlying reasons causing locomotor asymmetry, the inappropriate motor output and the lack of somatosensory feedback from the prosthetic limb are probably most important (Hof et al., 2007; Kannape and Herr, 2014). To correct these motor and sensory deficits, it is necessary to establish a bidirectional communication interface between the nervous system and the prosthesis.

Recent studies have shown the feasibility of replicating tactile sensory feedback from the amputated, phantom limb by electrical stimulation to residual cutaneous nerves (Dhillon et al., 2004; Ortiz-Catalan et al., 2014; Tan et al., 2014; Davis et al., 2016; Graczyk et al., 2016). Myoelectric signals with built-in pattern recognition algorithms enable fine motor control in arm prostheses, even without any sensory feedback (Li et al., 2010; Tkach et al., 2014). Likewise, it might be possible to improve locomotor outcome measures (e.g., walking symmetry) by controlling a powered prosthesis or orthosis using myoelectric signals from residual or intact muscles (Sawicki and Ferris, 2009; Herr and Grabowski, 2012; Takahashi et al., 2015; Kannape and Herr, 2016).

Recent developments of bone-anchored lower limb prostheses have improved the load transmission to the skeletal system, range of motion, comfort, and osseoperception (Hagberg and Branemark, 2009; Juhnke et al., 2015; Leijendekkers et al., 2016). In addition, bone-anchored limb prostheses may potentially allow for a secure and stable neural interface between the residual nerves and muscles and the prosthesis (Pitkin et al., 2012; Al-Ajam et al., 2013; Ortiz-Catalan et al., 2014).

We have used rodent and feline animal models to test integration of skin-and-bone integrated pylons (SBIP) with the residual tissue (Pitkin et al., 2009; Farrell et al., 2014b,c; Jarrell et al., 2018). These studies have demonstrated the potential of the SBIP implant to provide secure, infection-free fixation of the prosthesis to the residual limb. This type of implant can also be used as a gateway for transmission of nerve and myoelectric signals between the residual limb and prosthesis (Pitkin et al., 2012). For example, pressure applied to the prosthesis during the stance phase of walking can be transmitted to the nervous system via electrical stimulation of residual cutaneous nerves (Park et al., 2015, 2016), whereas myoelectric activity recorded in residual muscles can be used to drive prosthetic actuators.

Although bone-anchored powered transtibial prostheses integrated with sensory and motor nerve fibers or muscles via a percutaneous pylon have the great potential for improving quality of prosthetic locomotion as discussed above, there have been no rigorous studies on animal models that tested the feasibility and performance of such prostheses. Prior to implementing this technology in people with limb loss, preclinical animal studies should address the following important questions: (i) Do these prostheses improve symmetry of locomotion and to what extent? (ii) How does continual electrical stimulation of peripheral nerves affect the nerve structural integrity and function? (iii) Does stimulation of sensory nerves engage proper reflex responses and how they change over time? (iv) Do residual muscles and their myoelectric activity controlling prosthetic actuators degrade over time to a degree that cannot be compensated by the control system? (v) Does the porous titanium implant serving as a prosthesis-body gateway allow for skin ingrowth and reduction of the infection rate, etc.

The use of animal models for testing sensing, powered prostheses during locomotion may be challenging. The first challenge is securing a limb prosthesis on the animal. Rodents, cats, and dogs are notorious for removing externally attached assistive devices (Mich, 2014); therefore, the use of bone-anchored implants for prosthesis attachment appears a viable option (Fitzpatrick et al., 2011; Farrell et al., 2014b; Jarrell et al., 2018). Another challenge is strict limitations on prosthesis small size and mass and a relatively high power output. For the cat of 3 to 4 kg, for example, the half of tibia length is approximately 55 mm (Klishko et al., 2014); mass of the foot with half of the shank is ~80 g (Hoy and Zernicke, 1985); the average peak of the ankle moment during level walking is 0.73–0.75 Nm (Gregor et al., 2006; Prilutsky et al., 2011); and the average peak of ankle positive power in the same conditions is 0.86 W (Prilutsky et al., 2011). Thus, each component of the prosthesis [prosthetic foot, sensors, actuator, battery, neural stimulator and amplifier, microprocessor unit (MCU), and electronics] should be carefully selected to satisfy these requirements. ABS plastic, carbon fiber, or fiberglass are lightweight materials with high ultimate strength and can be used for prosthetic foot fabrication (Delussu et al., 2013; Farrell et al., 2014b; Corbett et al., 2018). Options for appropriate prosthetic actuators and batteries are more limited as they need to satisfy the conflicting requirements for lightweight and high power output. Soft pneumatic actuators, satisfying the above requirements, have been recently developed and used in limb prosthetic and orthotic applications in people and animals (Ferris et al., 2005; Roche et al., 2014; Florez et al., 2017). However, these actuators require large off-board air pressure regulators and therefore are better suited for rehabilitation and research of assisted locomotion on a treadmill. Linear electromechanical actuators has demonstrated sufficient power production in relatively light wearable, powered prosthetic ankles during human walking (Blaya and Herr, 2004; Garcia et al., 2011; Realmuto et al., 2011). Considering the above limitations on size, weight, and moment production for the cat prosthetic ankle, a miniature linear actuator (PQ12-63-06-P, Actuonix, BC, Canada) appears to be a good choice. With its small weight of 15 g, stroke length of 20 mm, and maximum force of 45 N, it should produce an extension ankle moment of ~1 Nm with the moment arm of ~0.025 m corresponding to that of the cat Achilles tendon (Prilutsky et al., 1996). A further challenge is the selection of an appropriate feedback control law for the prosthesis. Although a wide variety of feedback control laws are employed by terrestrial animals including humans during locomotion (Edwards and Prilutsky, 2017), proportional-derivative control laws are often used in orthotic-prosthetic ankle emulators controlled by powerful off-board electric motors or pressure regulators to reproduce either the desired joint moment or joint position (Sawicki and Ferris, 2009; Caputo and Collins, 2014). In wearable powered prostheses, finite-state controllers are often used that do not require exact tracking of a desired joint moment or angular trajectory (Au et al., 2007; Shultz et al., 2016) and thus permit the use of lighter and less powerful actuators.

The goal of this work was to develop and benchtop characterize a prototype of a bone-anchored, powered, and sensing transtibial prosthesis for a feline animal model of prosthetic gait. The developed prototype included an ABS plastic foot with force sensor, stimulator of a sensory nerve, EMG amplifier, linear actuator, battery, and microprocessor. The prototype satisfied the design criteria for prosthesis weight and moment production. In benchtop testing, the performance of a finite-state control scheme for the prosthesis was evaluated by subjecting the prosthesis to rhythmic loading that simulated the stance and swing phases of locomotion. A force sensor on the ground detected two motion states – the stance and swing, and the linear actuator generated an extension and flexion moment, respectively. An empirical relationship between muscle activity and ankle moment developed using our previous data were simplified by a step function with a variable gain. The gain of the extension moment was adjusted in each cycle automatically via a wireless interface and off-board PC to reduce the error between the desired peak of the ground reaction force (GRF) and the measured peak. The prosthetic prototype was able to reproduce the desirable GRF peaks within several cycles.

MATERIALS AND METHODS

Prosthesis Design

Prosthesis Components

The prosthesis comprised (1) MCU, (2) EMG amplifier, (3) current stimulator, (4) force-position sensor, (5) linear actuator, (6) battery and coil, (7) power management, and (8) prosthetic foot. (1) The MCU model CC2510F32 (Texas Instruments, TX, United States) included 8051 microcontroller and wireless transceiver with low-power consumption. (2) EMG amplifier INA128 with gain of 1000 (V/V) (Texas Instruments, TX, United States) included an embedded Sallen-Key active band-pass filter to suppress both motion artifact and ambient noise. (3) Current stimulator had discrete n-type field effect transistors (nFETs) and p-type field effect transistors (pFETs) designed to generate biphasic current pulses, while a programmable resistor AD5162 (Analog Devices, MA, United States) adjusted the current level of the pulses using current steering. The stimulator was tested in walking cats – electrical stimulation was applied to the distal tibial nerve during the stance phase of walking and reduced or reversed effects of paw pad anesthesia on the duty factor and step length symmetry (Park et al., 2015, 2016). (4) ThinPot linear force-position sensor (Spectra Symbol, UT, United States) was fixed on the bottom of the J-shaped foot, between the J-shaped plastic foot and the rubber layer. The sensor can record normal force with the 1-bit resolution at a threshold of 0.7 N. This is sufficient to detect paw contact during walking in cats (Park et al., 2015, 2016). (5) A miniature linear actuator PQ12-63-06-P (Actuonix, BC, Canada) with a brushed DC motor and transmission gear with a 63:1 ratio can produce a 20-mm stroke, which corresponds approximately to muscle-tendon unit length changes of a cat ankle extensor (soleus, SO) during locomotion (Gregor et al., 2006). This single linear actuator with an H-bridge motor driver (DRV8837, Texas Instruments, TX, United States) could extend and flex the prosthetic joint and thus reproduce actions of the ankle extensors (e.g., SO) and flexors (e.g., tibialis anterior, TA). (6) A Li-polymer rechargeable battery GM053040 (550 mAh, 5 mm $\times$ 30 mm $\times$ 40 mm) was selected as the power source. Its maximum discharge current (550 mA) corresponds to the maximum stall current of the linear actuator PQ12-63-06-P. We estimated the battery would last before recharging for 1.5 h based on current requirements of the linear actuator to generate force of 20 N ($\sim$200 mA), current requirements for other electronic components ($<$20 mA), the DC–DC conversion ratio ($\sim$2:1) and efficiency ($\sim$85%), and walking duty cycle ($<$75%). The inductive coil was provided for wireless recharging. (7) Power management generated 3V outputs for the MCU and foot force-position sensor, 5 V outputs for the EMG amplifier and current stimulator, and a 6 V output for the linear actuator. (8) J-shaped foot was 3D printed from the ABS plastic capable of withstanding forces of 60–90 N that exceed peak ground reaction forces (GRF) during cat walking by two to three times (Corbett et al., 2018). The diagram in **Figure 1** illustrates the signal and power flow between the prosthetic components. The signal flow from the ThinPot linear force-position sensor on the foot (4) to the current stimulator (3) represents the sensory pathway (green arrows), whereas the signal flow from the EMG amplifier (2) to the linear actuator (5) – the motor pathway (blue arrows).

The prosthesis was wirelessly connected with external devices, i.e., a force sensing resistor FSR406 (Interlink Electronics, CA, United States) mounted on the floor and a computer monitoring GRF and adjusting a motor gain of the linear actuator in real time. An external MCU with a wireless transceiver and microcontroller provided communications between the external devices (**Figure 2**) and the prosthesis.

Prosthesis Assembly

A rectangular aluminum bar (6061-T6511, Metalsdepot, KY, United States) 55 mm in length served as a structural frame for the prosthesis (**Figure 3**). The bar was connected to the J-shaped plastic foot via a pivot. The aluminum bar was also connected to the percutaneous pylon that would be implanted into the medullary cavity of the cat tibia and interfaced with residual cutaneous nerves and SO and TA muscles via implanted electrodes.

The linear actuator (see above) was attached to a posterior side of the aluminum bar at a 25-mm distance from the ankle pivot (this distance approximately corresponds to the moment arm of the cat Achilles tendon with respect to the ankle (Goslow et al., 1973; Prilutsky et al., 1996). Two separate printed circuit boards (PCBs) were placed to the right of the linear actuator and the flat part of the J-shaped foot. The MCU, wireless interface, EMG amplifier, and power management integrated with the PCB were placed to the right of the linear actuator. The motor driver, sensor interface, and stimulator integrated with the PCB were fixed on the flat part of J-shaped foot. Finally, a Li-polymer rechargeable battery was mounted to the left of the linear actuator.

The prosthesis components were selected to satisfy the design criteria for prosthesis weight and moment production. As a result, the prosthesis mass was 63 g with the maximum available moment (stall moment) of 1 Nm. The stall moment was calculated from the maximum push/pull force of the linear actuator (40 N) and the actuator moment arm with respect to the pivot (note that we measured the maximum force of the linear actuator and the obtained value of 40 N was slightly lower that

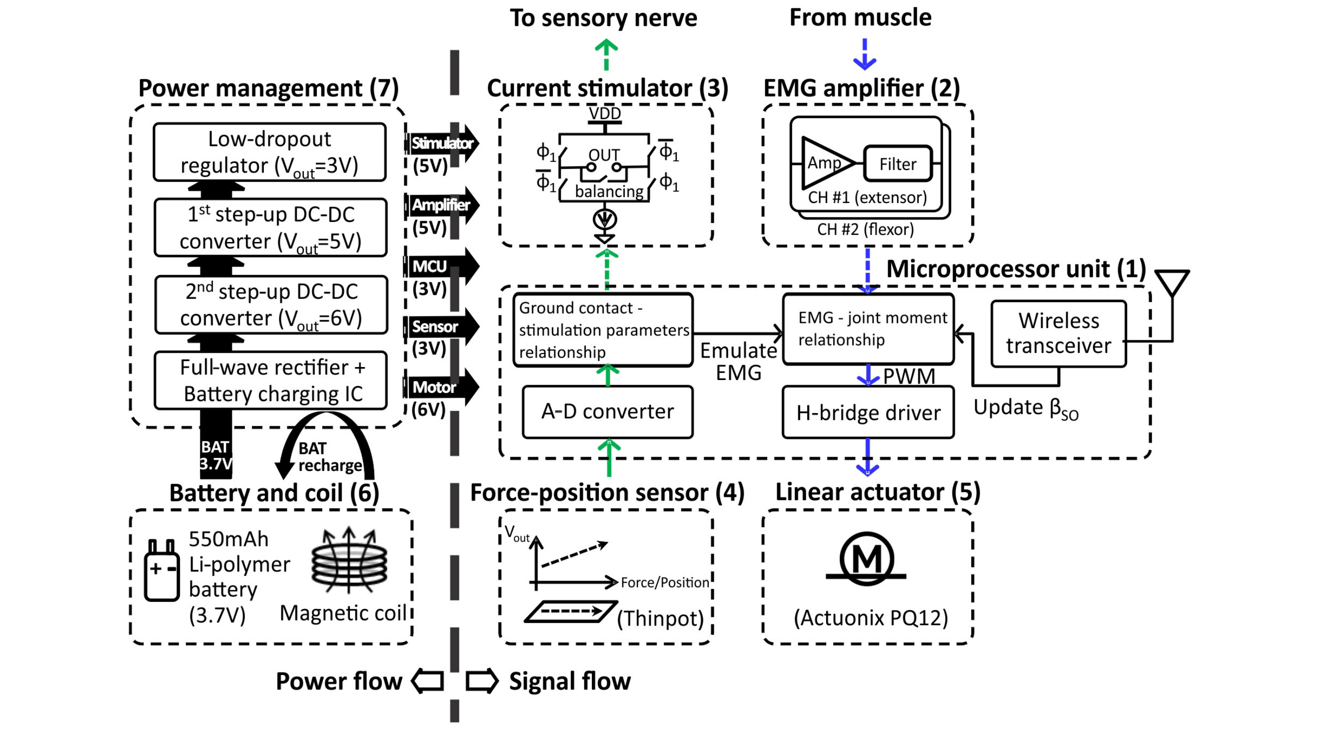

FIGURE 1 | Block diagram illustrating power flow (on left) and signal flow (on right) between prosthetic components. The sensory pathway of signal flow on right is indicated by the green arrows; the motor pathway is indicated by blue arrows. The pathways represented by dashed arrows are not implemented in the prosthetic prototype, but will be implemented when the prosthesis is worn by the cat. See text for details.

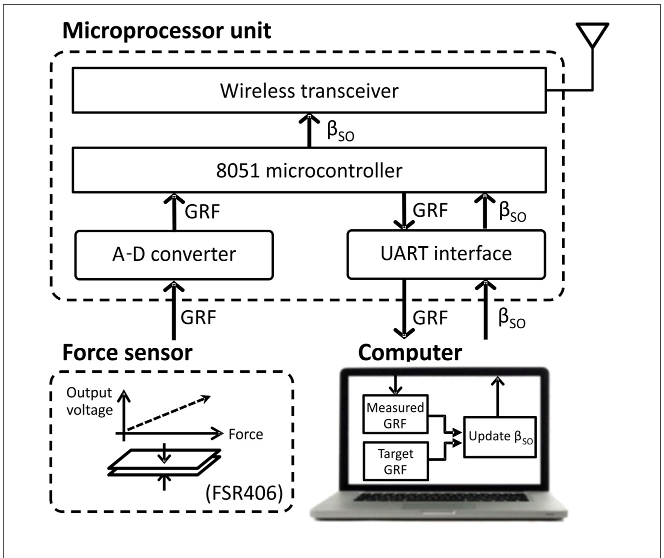

FIGURE 2 | Block diagram of external devices (computer, ground force sensor, and microprocessor unit) that update the extension gain β_{SO}, based on the ground reaction force (GRF) peak, and transmit it wirelessly to the prosthesis. See text for details.

45 N reported by manufacturer). The value of 1 Nm is close to the maximum ankle moment during level walking in the cat (McFadyen et al., 1999; Gregor et al., 2006; Prilutsky et al., 2011).

Prosthesis Control

Finite-State Controller

A simple finite-state machine controller was implemented to control the linear actuator (**Figure 4A**). Transitions between the two states – stance and swing – depended on the presence of contact with the ground and EMG activity of a residual ankle extensor and flexor muscles. Transition from the stance to swing state was triggered by (i) foot unloading (interruption of contact with the ground), (ii) terminating EMG activity of the ankle extensor, and (iii) initiating EMG activity of the ankle flexor (**Figure 4A**). These three conditions triggered a pushing stroke of the linear actuator leading to a flexor moment at the ankle. Transition from the swing to stance state was initiated by (i) onset of ground contact with the foot, (ii) onset of EMG activity of the ankle extensor, and (iii) offset of EMG activity of the ankle flexor. These conditions triggered a pulling stroke of the linear actuator producing an extension ankle moment.

Ankle Moment–EMG Relationship

To modulate the output of the linear actuator during the stance and swing states of walking, we established a relationship between EMG activities recorded from ankle extensor and flexor muscles and the resultant ankle moment (motor pathway, **Figure 1**).

The relationship between EMG activity of an ankle extensor SO and ankle flexor TA and ankle moment during level walking in the cat was obtained from previously recorded EMGs and ankle moment (Prilutsky et al., 2011;

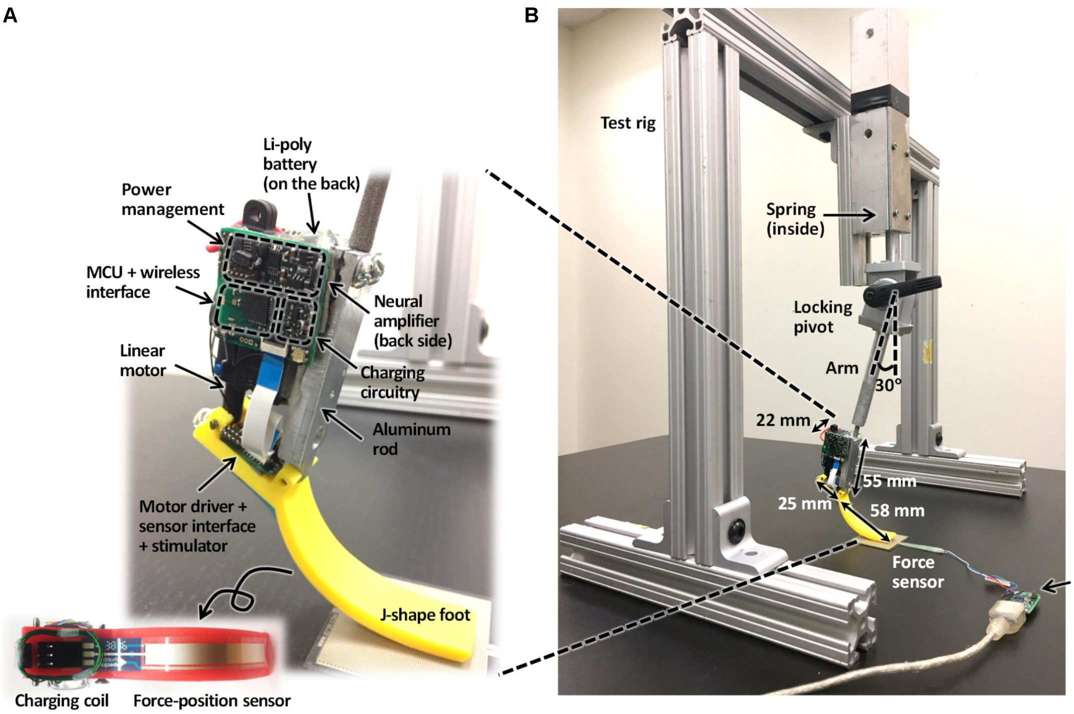

FIGURE 3 | Prosthesis prototype **(A)** and test rig with the attached prosthesis **(B)**.

Markin et al., 2012) using a multivariate linear regression analysis in software STATISTICA 7 (StatSoft, United States). The equation had the following form (Prilutsky et al., 2005):

$$M_{ANK}(t) = \beta_0 + \beta_{SO} EMG_{SO}(t - \Delta t) + \beta_{TA} EMG_{TA}(t - \Delta t), \tag{1}$$

where M_{ANK} is the ankle joint moment in Nm; EMG_{SO} and EMG_{TA} are normalized EMG activities of SO and TA muscles, changing from 0 to 1; t is time and $\Delta t \approx 60$ ms is the electromechanical delay between the appearance of EMG activity and the onset of the resultant joint moment (Gregor et al., 2006); $\beta_o \approx 0$ (see Results), β_{SO} and β_{TA} are empirical constants (measured in Nm). Approximately two-thirds of total 22 walking cycles (n = 15) from three cats were randomly selected and used to derive regression equation (1). The remaining cycles (n = 7) were used to compare the predicted ankle moment M_{ANK} with the experimental one. The detailed description of how the joint moments and EMG activities were obtained and processed can be found in the original publications (Prilutsky et al., 2005, 2011; Markin et al., 2012).

Ground Contact Pressure and Tactile Perception

In our preliminary studies (Park et al., 2015, 2016), we have established the relationship between output of the force-position sensor under the cat hindpaw and electrical stimulation of the distal tibial nerve (sensory pathway, **Figure 1**) that apparently perceived by the cat as contact with the ground during walking. When the output of the force sensor exceeded a threshold (indicating the stance phase), the current stimulator delivered stimulation (trains of 200-μs biphasic rectangular pulses, 100 Hz, 1.2 T) to the distal tibial nerve. This sensory nerve stimulation reduced or reversed effects of local anesthesia of the ipsilateral hind- and forepaws on the step length symmetry and duty factor (Park et al., 2015, 2016).

Implementation of Control During Benchtop Testing

For benchtop testing of the developed prosthesis outside the animal in this study, both the sensory and motor pathways were simplified. The simplified sensory pathway transmitted information about the timing of ground contact, measured by the force-position sensor on the foot, to the linear actuator instead of the current stimulator (**Figure 1**). The timing of ground contact was described as a unit step function $S(t)$:

$$S(t) = H(F(t) - F_{TH}), \tag{2}$$

where $F(t)$ is the recorded force-position sensor output, F_{TH} is the force detection threshold, and $H(x)$ is a Heaviside step function, i.e., $H(x) = 1$ if $x > 0$ and $H(x) = 0$ if $x \leq 0$. Function $S(t)$ defined the stance and swing phases (finite states of the system; **Figure 4A**), and this phase information was used to emulate a simplified motor pathway, i.e., the relationship between the ankle moment and EMG of SO and TA muscles. Specifically, EMG activity of SO and TA muscles was emulated by unit step functions representing the timing of muscle activity derived from the ground contact information. SO EMG was computed as

$$EMG_{SO}(t) = S(t - \Delta t_{SO}) - S(t - (\Delta t_{SO} + T_{SO})), \tag{3}$$

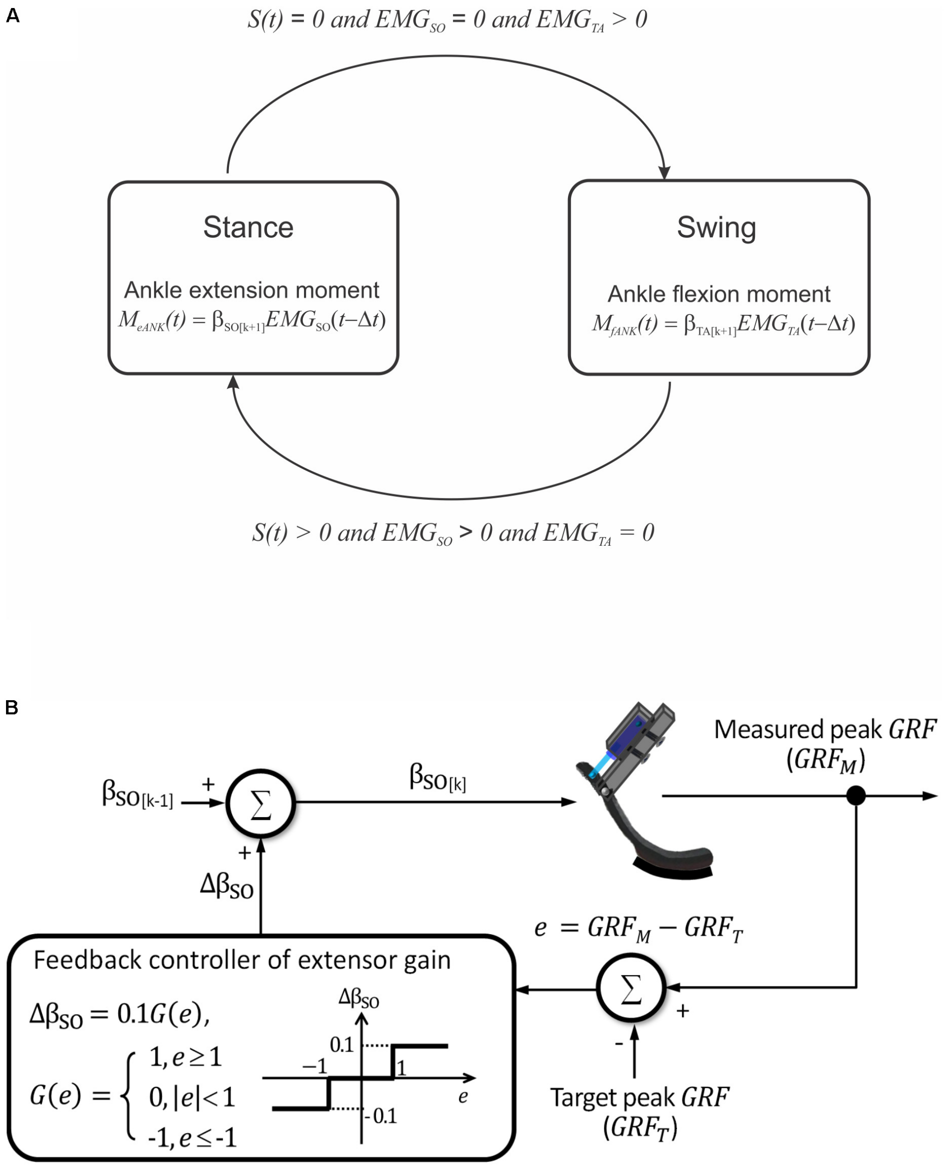

FIGURE 4 | Schematics illustrating prosthesis control. **(A)** Two finite states of prosthesis loading and conditions for transitions between them. *S*(*t*) is a step function indicating presence [*S(t)* > 0] or absence [*S(t)* = 0] of ground contact. EMG_{SO} and EMG_{TA} are step functions indicating presence or absence of EMG activity in ankle extensor soleus (SO) and ankle flexor tibialis anterior (TA), respectively. **(B)** Closed-loop modulation of extension gain b_{SO}. The gain is changed by 10% in each cycle *k* depending on the value of error *e* between the measured and target peaks of ground reaction force (GRF).

where Δt_{SO} is the phase delay between the previous stance phase offset and subsequent SO EMG onset, T_{SO} is the duration of EMG_{SO} activity, *S(t)* is the step function representing contact information (see Eq. 2). In the tests described here, the following parameters of Eq. 3 were used (Prilutsky et al., 2005, 2011; Markin et al., 2012): Δt_{SO} = 100 ms and T_{SO} = 500 ms.

TA EMG activity was computed as

$$EMG_{TA}(t) = S(t - \Delta t_{TA}) - S(t - (\Delta t_{TA} + T_{TA})) \qquad (4)$$

where Δt_{TA} is the phase delay between the previous stance phase onset and subsequent TA EMG onset, T_{TA} is the duration of EMG_{TA} activity; $\Delta t_{TA} =$ 400 ms and T_{TA} = 200 ms (Prilutsky et al., 2005, 2011; Markin et al., 2012).

The emulated EMG signals (Eqs 3 and 4) were used to control the linear actuator with a dual polarity. The ankle joint moment was calculated using Eq. 1 and emulated EMG activity of SO and TA obtained from Eqs 3 and 4 (**Figure 4A**). Because SO and TA during walking have reciprocal activity and β_0 is close to zero (see Eq. 1 and Results), calculations of the ankle extension and flexion moments were simplified as $M_{e\,ANK}(t) = \beta_{SO}\,EMG_{SO}(t - \Delta t)$, and $M_{f\,ANK}(t) = \beta_{TA}\,EMG_{TA}(t - \Delta t)$, respectively (see **Figure 4A**). In these equations, β_{SO} and β_{TA} are extension and flexion motor gains.

Closed-Loop Updates of Extension Motor Gain

The maximum of extension gain β_{SO} was set at 1 Nm. The updated value of the gain in a next cycle could be increased or decreased by 10% depending on the difference $e = GRF_M - GRF_T$ between the measured GRF peak (GRF_M) and a target GRF peak (GRF_T), respectively, in the current cycle (**Figure 4B**):

$$\beta_{SO[K]} = \beta_{SO[K-1]} + 0.1\,G(e) \qquad (5)$$

where k is the cycle number and $G(e) = 1 \, if \, e \geq 1$, $G(e) = 0 \, if \, |e| < 1$, $G(e) = -1 \, if \, e \leq -1$. Thus, if the GRF_M exceeded or was less than the target value by 1 N or more, the current extension gain would be decreased or increased by 10%, respectively; otherwise, the gain would not change (**Figure 4B**).

Benchtop Characterization of Prosthesis

During the benchtop characterization, we imposed rhythmic loading on the prosthesis to simulate the stance and swing phases of walking and to test the finite-state machine controller (**Figure 4A**) with a closed-loop modulation of the extension gain in real time (**Figure 4B**).

Design of a Test Rig

To perform benchtop characterization, we designed a test rig made of aluminum bars with L-shaped connectors, a zinc-plated compression spring, locking pivot, and prosthesis support arm (**Figure 3B**). The force produced by the compressed spring, along with the weight of the prosthesis and its support arm, caused loading of the prosthesis during contact with the ground that was comparable to GRF exerted by the hindpaw during normal level walking in the cat. The support arm was set at a vertical angle of 30° so that the J-shaped prosthetic foot could be in contact with the ground starting at both full flexion (at foot contact) until full extension (foot off) of the ankle joint.

Test Procedure

Each test cycle started from onset of the swing state of the controller – the prosthesis foot was positioned just above the ground, prosthetic ankle was fully extended, and the linear actuator started producing a flexion ankle moment. This prosthesis position corresponded to full relaxation of the compression spring. The researcher raised the prosthesis by the hand to a height of ~40 mm, at which the spring was fully compressed, and then the prosthesis was released. The fully compressed spring accelerated the prosthesis toward the ground vertically. Given spring deformation of ~40 mm and stiffness of 0.36 N/mm, the spring applied ~14 N to the prosthesis when it was released by the hand.

When the prosthesis touched the ground, the foot force-position sensor detected the ground contact and the conditions for the swing to stance state transition were satisfied: $S(t) > 0$ (Eq. 2), $EMG_{SO} > 0$ (Eq. 3), and $EMG_{TA} = 0$ (Eq. 4). At that instant, the linear motor initiated a pull stroke and generated extension ankle moment (M_{eANK}, see **Figure 4A**). When the prosthetic joint reached the maximum extension at the end of stance phase, the prosthesis was lifted by the experimenter's hand and raised against the compression spring as described above. As soon as ground contact was lost, the conditions for the stance to swing state transition were satisfied: $S(t) = 0$ (Eq. 2), $EMG_{SO} = 0$ (Eq. 3), and $EMG_{TA} > 0$ (Eq. 4). At that instant, a flexion ankle moment was generated (M_{fANK}, see **Figure 4A**), and the prosthesis joint angle returned to the fully flexed position. Cadence of prosthesis loading in these tests corresponded to a typical cadence of walking cats (Gregor et al., 2006).

We also tested the ability of the feedback controller to modulate the extension gain β_{SO} and thus the magnitude of the exerted ankle moment (M_{eANK}, **Figures 4A,B**) in real-time. The produced peak GRF (GRF_M) was measured by the force sensor FSR406, mounted on the ground under the prosthesis foot (**Figure 3B**). The target value of GRF_T was set and compared with the GRF_M value in a custom designed LabView (National Instruments, TX, United States) application on the off-board computer. Based on the operating principle of the DC motor, we assumed that the extension gain β_{SO} (and thus extension moment M_{eANK}) was proportional to the duty cycle of pulse-width modulation (PWM) of control signal (Weber, 1965). The maximum value of extension gain (β_{SO} = 1 Nm) corresponded to the extension ankle moment M_{eANK} = 1 Nm and PWM = 100%. With this maximum gain, the linear actuator produced the maximum force of 40 N and could generate the maximum ground reaction peak of ~13–15 N (see Results). The extension gain β_{SO} (corresponding to PWM) was updated in each test cycle based on Eq. 5 (**Figure 4B**). The closed-loop control system was tested at three target values of GRF_T: 14, 6, and 12 N. These three target forces were pre-programmed in the microprocessor to occur at the onset of testing, at the end of cycle 2 and at the end of cycle 8, respectively. During testing, the flexion gain β_{TA} was set at the maximum value of −1 Nm and not changed (**Figure 4A**).

RESULTS

Ankle Moment-EMG Relationship

Rectified and low-pass filtered EMG activities of SO and TA, as well as the corresponding ankle joint moments, recorded in Prilutsky et al. (2011), Markin et al. (2012) during 22 cycles of level walking in three cats (**Figures 5A–C**), were used to obtain the regression Eq. 1. The empirical constants in Eq. 1 were β_0 = 0.023528 Nm, β_{S0} = 0.969663 Nm, and β_{TA} = 0.052416 Nm. The coefficient of multiple correlation for Eq. 1 was r = 0.874 ($p < 0.05$). The ankle moment as a function of the normalized cycle time computed from SO and TA EMGs using Eq. 1 was generally within one standard deviation from the mean experimental moment (**Figure 5D**). As explained in Materials and Methods, SO and TA EMG activity was simplified for the purpose of the benchtop testing of the prosthesis by step functions EMG_{SO} and EMG_{TA} (Eqs 3 and 4). These step functions are shown in **Figures 5A,B** by red dashed rectangles.

Finite State Controller With Closed-Loop Update of Extension Gain

During rhythmic loading of the prosthesis, the finite state controller correctly identified the stance and swing states based

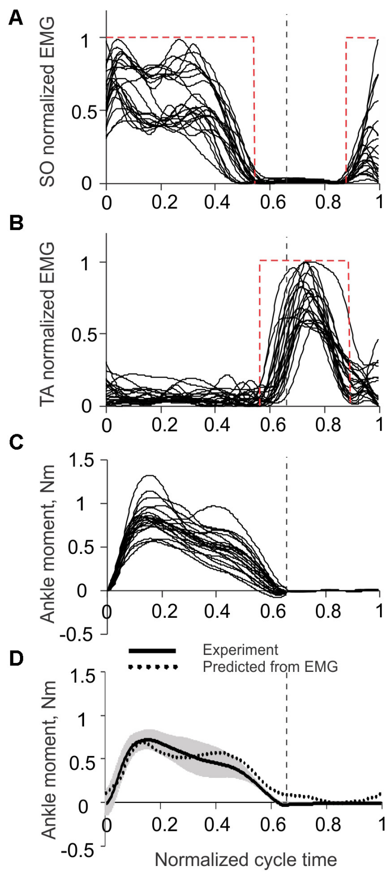

FIGURE 5 | Ankle joint moment and EMG activity of soleus (SO) and tibialis anterior (TA) muscles during level walking in the cat. The vertical dashed lines separate the stance and swing phases. Experimental EMG and ankle moment data are taken from 22 cycles of level walking of three cats (mass 3.55 ± 0.65 kg; mean ± SD) (Prilutsky et al., 2011; Markin et al., 2012). **(A)** Normalized SO EMG during level walking in the cat. The red dashed rectangle corresponds to emulated SO EMG signal (see text for details). **(B)** Normalized TA EMG during level walking in the cat. The red dashed rectangle corresponds to emulated TA EMG signal (see text for details). **(C)** Ankle joint moment during level walking in the cat; positive values correspond to extension (plantar flexion). **(D)** Ankle moment obtained experimentally (solid line with gray shade, mean ± SD) and predicted from SO and TA EMGs using Eq. 1 (dotted line). Positive values correspond to extension (plantar flexion).

on the signal from the force-position sensor on the bottom of the foot. The linear actuator produced pulling strokes (extension ankle moments) in the stance state and pushing strokes (flexion moments) in the swing state. In the example in **Figure 6A**, the prosthesis produced GRF in 14 cycles of rhythmic loading; the corresponding changes in the PWM duty cycle are shown in **Figure 6B**. In the first two cycles, the target GRF force was 14 N, which corresponded to the maximum capacity of the linear actuator (PWM duty cycle was 100%). Since the GRF peaks produced in these cycles were within ±1 N of the target value, the extension gain β_{SO}, and PWM were not changed (**Figure 6B**, Eq. 5). At the end of stance phase of cycle 2, when the target force was reduced from 14 to 6 N, the force error e (Eq. 5) was detected in stance of cycle 3 and the extension gain β_{SO}, and PWM were reduced by the control system by 10% in cycles 4 through 6 until the peak GRF error during stance became smaller than 1 N in cycle 7 (**Figure 6**). The peaks of GRF in cycles 7 and 8 were maintained near the target force of 6 N within ±1 N, and no changes in PWM occurred. After the target force changed at the end of cycle 8 from 6 to 12 N, the controller detected the force difference e in stance of cycle 9 and increased PWM by 10% in cycle 10. Since the measured GRF peaks in cycles 10 and 11 were lower than the target value, PWD was increased again by 10% in cycles 11 and 12. Since the GRF peaks in cycles 13 and 14 were within ±1 N from the target value of 12 N, no changes in PWD occurred in these cycles (**Figure 6**).

The peak GRF values during the transition period from the target change to achieving the target by the system (cycles 3 through 7 and 8 through 12; **Figure 6A**) could be considered the system step response to the error e input (**Figure 6B**). In the current control system design, the response time corresponded to the duration of one cycle. The prosthesis closely reproduced the target GRF peaks in steady state cycles 1–3, 7–9, and 12–14 (**Figure 6A**). The absolute error of peak GRF across all three target values was 0.31 ± 0.23 N (mean ± SD), and the relative error (absolute error normalized to the target value) was 3.49 ± 3.06%.

Ground Reaction Forces Produced by the Prosthesis

The time profiles of GRF measured under the prosthetic foot in 14 consecutive cycles had a double-peak pattern (**Figure 6A**). The mean GRF peak in cycles 1 through 3, where the PWM duty cycle was set to 100% to produce maximal GRF peaks, was 13.8 ± 0.5 N. This value was within one standard deviation of the GRF mean peak (14.9 ± 1.6 N) obtained in walking cats (**Figure 7**).

The comparison of the prosthetic GRF profiles averaged across cycles 1 through 3 with the experimental GRF recorded previously during level walking in cats (Prilutsky et al., 2011) – the same 22 cycles from which ankle moments and EMG patterns in **Figure 5** were obtained, demonstrated close qualitative and quantitative agreements (**Figure 7**). Specifically, both patterns had two peaks – one in the early stance phase (leg contact) and the other one in the late stance phase.

DISCUSSION

We developed a powered, sensing transtibial prosthesis for the use in the feline animal model of prosthetic gait. This animal model is needed for testing feasibility and performance of bone-anchored limb prostheses integrated with residual sensory nerves and muscles during locomotion (see Introduction). The size, mass, and maximum extension moment of the prosthesis closely matched the corresponding parameters of the cat foot-ankle with the distal shank and the peak ankle extension moment produced during level walking in the cat (Gregor et al., 2006, 2018; Prilutsky et al., 2011). The prosthetic powered ankle joint was designed for control of the linear actuator by the recorded EMG activity of the residual ankle extensor and

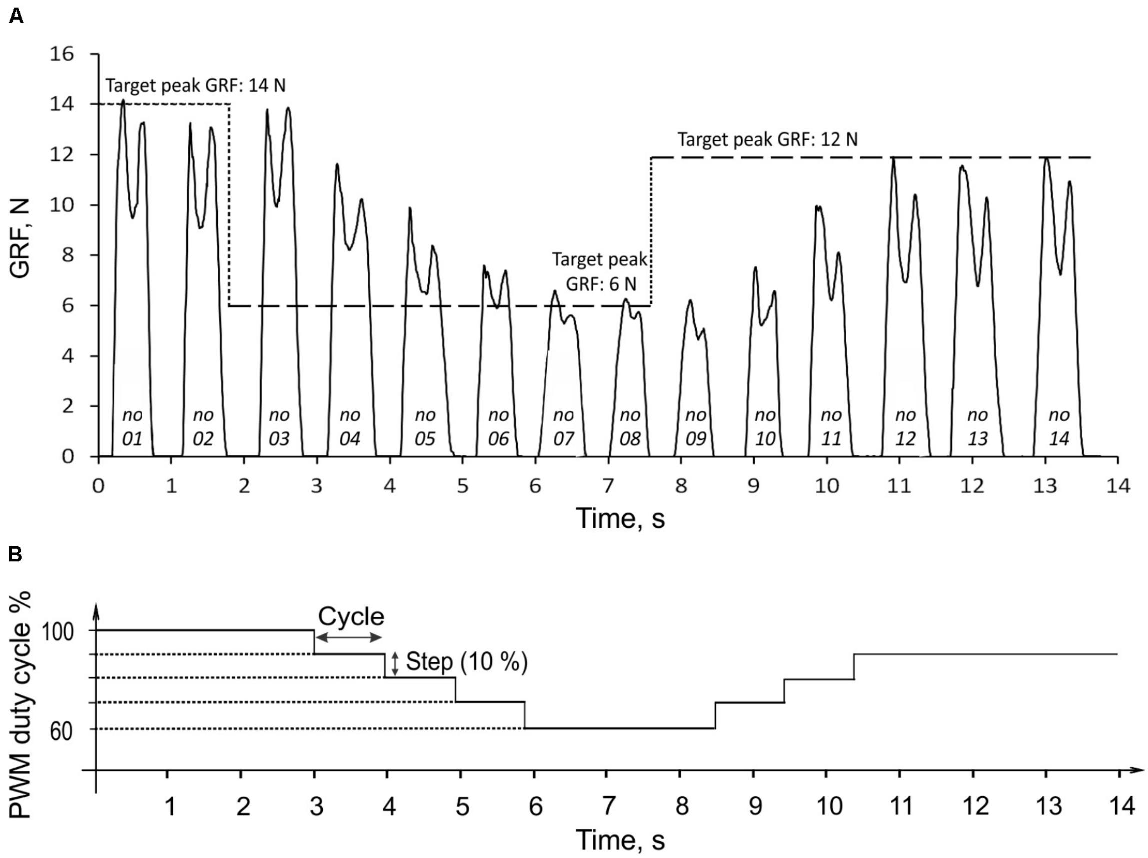

FIGURE 6 | Ground reaction force (GRF) during 14 cycles of prosthesis loading **(A)** and the corresponding changes in PWM duty cycle of the actuator **(B)**. The three target values of GRF peak (14, 6, and 12 N) are indicated by the horizontal dashed lines in **(A)**. The numbers at bottom of force traces indicate the cycle number. For details, see text.

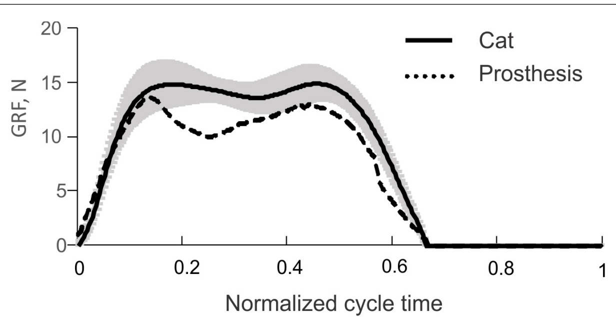

FIGURE 7 | Vertical ground reaction force (GRF) recorded during level walking in the cat (solid line and shade, mean ± SD; computed using data from Prilutsky et al., 2011) and mean GRF recorded during the first three cycles of prosthesis testing (dashed line), see **Figure 6A**.

flexor muscles. The ability of the prosthesis to detect timing of ground contact will allow for delivering tactile sensory feedback by phase dependent stimulation of sensory nerves. The foot force-position sensor detecting touch with the ground in this study was used in the past to trigger electrical stimulation of the distal tibial nerve during the stance phase of walking and to provide tactile feedback to the nervous system of walking cats with the anesthetized hindpaw (Park et al., 2015, 2016).

In the present benchtop testing of the prosthesis, only selected prosthesis functions were characterized. They included detecting timing of ground contact onset and offset, control of transitions between the stance and swing states by the finite-state machine controller, and a real-time automatic modulation of the extension gain based on the measured GRF peak in each loading cycle (**Figure 4**). The results of testing demonstrated that the prosthesis was able to produce the extension and flexion ankle moments in the appropriate loading states. The prosthesis was also able to generate appropriate GRF peaks by modulating the extension gain in a closed-loop real time control. In addition, the prosthesis was capable of generating realistic GRF forces similar to those observed during normal level walking in the cat. Although the maximum GRF peaks were slightly lower than the desired value of 15 N (a typical GRF peak during level walking in the cat) and much lower than peak forces during 27°-upslope walking (17-22 N; Gregor et al., 2006; Prilutsky et al., 2011), we expect that proximal joints may be able to compensate for this difference during cat walking with the powered prosthesis. This expectation is based on a recent study demonstrating that cats walking with a passive bone-anchored transtibial prosthesis with no active ankle extension are able to generated ∼70 and ∼50% of the normal GRF peak observed in intact level and 27°-upslope walking, respectively (Jarrell et al., 2018).

The double-peak GRF profiles generated by the prosthesis (**Figure 6**) were not expected because the control system was designed to reproduce just a target GRF peak. It appears that the observed GRF profile is a result of interactions between the constant moment produced by the linear actuator and passive dynamics of the prosthesis and its support system. The two GRF peaks had different magnitudes, and the second peak was lower than the first (**Figure 6**).

The magnitude of the second peak of vertical GRF depends on the magnitude of ankle extension moment in the late-stance phase of prosthetic walking in humans. For example, reduction in passive foot stiffness leads to a parallel decrease in the second GRF peak and ankle extension moment peak (Fey et al., 2011). The use of powered ankle prostheses decreases or eliminates the differences in second GRF peak and ankle extension moment magnitude between the intact and prosthetic limbs in humans (Rabago et al., 2016; Shultz et al., 2016). Since our powered prosthesis with its control system is designed to maintain a target GRF peak, we do not expect a close match of the generated GRF profile with that of the intact animal. This expected mismatch should not necessarily lead to asymmetric walking unless there is a substantial mismatch in the GRF impulse.

The linear actuator PQ12-63-06-P was selected for the cat transtibial prosthesis because it satisfied strict limitations on the size and mass of the cat foot-ankle and distal shank. To maximize the force output of the actuator to ensure it could produce its maximum moment of 1 Nm, we increased its duty cycle from its optimum value of 20%, recommended by the manufacturer as the most efficient, to 100%. We verified consistency of the actuator operation with the duty cycle of 100% over multiple cycles in our benchtop prosthesis testing. We found that this linear actuator at the duty cycle of 100% could generate consistent levels of GRF for over 100 cycles. This number of cycles is sufficient for a single recording session in the cat.

It may be necessary to increase the moment arm of the linear actuator with respect to ankle joint or replace this actuator with a larger one if testing in the animal would demonstrate its inability to generate sufficient ankle moment and power. However, a larger size of the actuator and battery would increase demands on the knee and hip flexor muscles during the swing phase of walking and could lead to abnormal asymmetric locomotor pattern.

In our benchtop testing of the prosthesis prototype, the force sensing resistor FSR406 mounted on the floor (**Figure 3B**) measured vertical GRF peaks, and the linear force-position sensor (ThinPot) attached to the bottom of the foot (**Figure 3A**) detected ground contact timing used to emulate extensor and flexor EMG bursts and determined onset-offset times of the linear actuator (**Figure 4A**). In the actual implementation of the prosthesis in the animal, we plan to mount the force-sensing resistor FSR406 or a similar one on the bottom of the prosthetic foot to serve both functions, i.e., detecting ground contact and measuring GRF peaks. In that case, wireless communication between the prosthesis and external computer will be used to monitor, modify, and record characteristics of the control system (target GRF peaks, actuator gains, stimulation parameters, EMG, etc.).

One potential limitation of the force-sensing resistor FSR406 for monitoring the peak GRF is that it can only measure the normal component of the 3D GRF vector (vertical component in this study, **Figures 6A**, **7**), although the other two GRF components are also important for accurate description of foot interaction with the ground (Aubin et al., 2008). During level cat walking, the normal peak GRF force exceeds the anterior-posterior and medial-lateral peaks by ∼5 and >10 times, respectively (Farrell et al., 2014a). Thus, the peak of the normal GRG component might still be used to monitor and modify the prosthesis output during level walking in the cat. However, during 27°-upslope cat walking the normal and tangential (in progression direction) peaks are comparable (Gregor et al., 2006, 2018; Prilutsky et al., 2011). Therefore, for this walking condition some modifications in the GRF target or control algorithm may be necessary.

In the animal testing, the GRF peak measured by the force sensor FSR406 on the foot in each walking cycle will be compared with a preset target value, and gains β_{SO} and β_{TA} will be changed in real time if necessary. Information about ground contact onset and offset determined by the same sensor will be used to control timing of electrical stimulation of the sensory nerves. We could use the timing of ground contact to control the linear actuator as demonstrated in this study. However, we plan to use recorded EMG signals from residual SO and TA to estimate the ankle moment (Eq. 1) and use either the estimated moment peak or moment profile for control of the linear actuator. Gains β_{SO} and β_{TA} could be modified based on the measured GRF peaks (**Figure 4B**) or/and predicted ankle moment peak. This type of control seems more intuitive for the user (Ortiz-Catalan et al., 2014; Kannape and Herr, 2016) since it includes a highly adaptive living system in the control of the prosthesis output.

In our planned animal studies, we will evaluate the contribution of sensory nerve stimulation to SO and TA EMG activity magnitude, to symmetry of walking and to other locomotor characteristics by comparing walking with and without phase dependent stimulation of sensory nerves. Changes in quality of EMG signals and in activation thresholds of sensory nerves [recorded action potentials in the sciatic nerve in response to stimulation of the distal tibial, sural or superficial peroneal nerves while the animal is sedated (Ollivier-Lanvin et al., 2011; Park et al., 2016)] will be determined over several months. During testing the prosthesis in the animal model, we plan to add another sensory feedback signal – contact force from the dorsal surface of the prosthetic foot. Another force sensor FSR406 will detect contact of the dorsal surface of the prosthetic foot with an external object and trigger electrical stimulation of the superficial peroneal nerve if the contact occurs in the swing phase of locomotion. The superficial peroneal nerve is a cutaneous nerve innervating skin on the dorsum of the foot (Crouch, 1969). Electrical stimulation of this nerve during swing elicits stumbling corrective response in the cat (Forssberg, 1979; Wand et al., 1980; Quevedo et al., 2005), which helps the animal avoid tripping by enhancing stepping over the obstacle.

In the end of the study, the animals will be euthanized and the residual limb with the porous titanium implant, residual muscles, and nerves with implanted electrodes will be harvested for histological analysis (Farrell et al., 2014b,c). This analysis will reveal the extent of skin and bone ingrowth into the percutaneous implant and integrity of implanted muscles and nerves. The results of our planned animal studies will inform future designs of transtibial prostheses integrated with the residual limb in people.

CONCLUSION

In conclusion, the designed prototype of a feline bone-anchored, sensing, powered transtibial prosthesis demonstrated the ability to reproduce values and patterns of the GRF observed during normal walking in the cat. The prosthesis dimensions, mass, and extension moment produced were similar to the corresponding characteristics of the cat. The prosthesis was designed for use with a porous titanium pylon implanted in tibia (Pitkin et al., 2012; Farrell et al., 2014b; Jarrell et al., 2018) that could serve as a gateway for transmission of feedback (from the prosthesis to the peripheral sensory nerves) and feedforward (from implanted muscle electrodes to the prosthetic actuator) signals between the prosthesis and the residual limb.

AUTHOR CONTRIBUTIONS

BP and SD did conception and design of research; HP, MI, BP, and SD did prosthesis design; HP, MG, AK, and PB did design of control algorithm; HP and MI did experimental recordings; HP analyzed data; HP, AK, and PB prepared figures. HP, MG, AK, BP, and SD interpreted results of experiments; HP and BP drafted manuscript; HP, MI, MG, AK, BP, and SD edited and revised manuscript and approved final version of manuscript.

FUNDING

The study was supported by U.S. Department of Defense Grant W81XWH-16-1-0791.

REFERENCES

Al-Ajam, Y., Lancashire, H., Pendegrass, C., Kang, N., Dowling, R. P., Taylor, S. J., et al. (2013). The use of a bone-anchored device as a hard-wired conduit for transmitting EMG signals from implanted muscle electrodes. *IEEE Trans. Biomed. Eng.* 60, 1654–1659. doi: 10.1109/TBME.2013.2241060

Au, S. K., Herr, H., Weber, J., and Martinez-Villalpando, E. C. (2007). Powered ankle-foot prosthesis for the improvement of amputee ambulation. *Conf. Proc. IEEE Eng. Med. Biol. Soc.* 2007, 3020–3026.

Aubin, P. M., Cowley, M. S., and Ledoux, W. R. (2008). Gait simulation via a 6-DOF parallel robot with iterative learning control. *IEEE Trans. Biomed. Eng.* 55, 1237–1240. doi: 10.1109/TBME.2007.908072

Blaya, J. A., and Herr, H. (2004). Adaptive control of a variable-impedance ankle-foot orthosis to assist drop-foot gait. *IEEE Trans. Neural Syst. Rehabil. Eng.* 12, 24–31. doi: 10.1109/TNSRE.2003.823266

Burke, M. J., Roman, V., and Wright, V. (1978). Bone and joint changes in lower limb amputees. *Ann. Rheum. Dis.* 37, 252–254. doi: 10.1136/ard.37.3.252

Caputo, J. M., and Collins, S. H. (2014). A universal ankle-foot prosthesis emulator for human locomotion experiments. *J. Biomech. Eng.* 136:035002. doi: 10.1115/1.4026225

Corbett, C. E., Allen, E. V., Prilutsky, B. I., and Childers, W. L. (2018). "CatWalk: a passive prosthetic foot for felines with a transtibial amputation," in *Proceedings of the Annual Meeting of the American Academy of Orthotists and Prosthetists*, (Washington, DC: American Academy of Orthotists and Prosthetists).

Crouch, J. E. (1969). *Text-Atlas of Cat Anatomy*. Philadelphia, PA: Lea & Febiger.

Davis, T. S., Wark, H. A., Hutchinson, D. T., Warren, D. J., O'neill, K., Scheinblum, T., et al. (2016). Restoring motor control and sensory feedback in people with upper extremity amputations using arrays of 96 microelectrodes implanted in the median and ulnar nerves. *J. Neural Eng.* 13:036001. doi: 10.1088/1741-2560/13/3/036001

Delussu, A. S., Brunelli, S., Paradisi, F., Iosa, M., Pellegrini, R., Zenardi, D., et al. (2013). Assessment of the effects of carbon fiber and bionic foot during overground and treadmill walking in transtibial amputees. *Gait Posture* 38, 876–882. doi: 10.1016/j.gaitpost.2013.04.009

Dhillon, G. S., Lawrence, S. M., Hutchinson, D. T., and Horch, K. W. (2004). Residual function in peripheral nerve stumps of amputees: implications for neural control of artificial limbs. *J. Hand Surg. Am.* 29, 605–615; discussion 616–608. doi: 10.1016/j.jhsa.2004.02.006

Edwards, D. H., and Prilutsky, B. I. (2017). "Sensory feedback in the control of posture and locomotion," in *Neurobiology of Motor Control: Fundamental Concepts and New Directions*, eds S. L. Hooper and A. Büschges (New York, NY: Wiley), 263–304.

Farrell, B. J., Bulgakova, M. A., Beloozerova, I. N., Sirota, M. G., and Prilutsky, B. I. (2014a). Body stability and muscle and motor cortex activity during walking with wide stance. *J. Neurophysiol.* 112, 504–524. doi: 10.1152/jn.00064.2014

Farrell, B. J., Prilutsky, B. I., Kistenberg, R. S., Dalton, J. F. T., and Pitkin, M. (2014b). An animal model to evaluate skin-implant-bone integration and gait with a prosthesis directly attached to the residual limb. *Clin. Biomech.* 29, 336–349. doi: 10.1016/j.clinbiomech.2013.12.014

Farrell, B. J., Prilutsky, B. I., Ritter, J. M., Kelley, S., Popat, K., and Pitkin, M. (2014c). Effects of pore size, implantation time, and nano-surface properties on rat skin ingrowth into percutaneous porous titanium implants. *J. Biomed. Mater. Res. A* 102, 1305–1315. doi: 10.1002/jbm.a.34807

Ferris, D. P., Sawicki, G. S., and Domingo, A. (2005). Powered lower limb orthoses for gait rehabilitation. *Top. Spinal Cord Inj. Rehabil.* 11, 34–49. doi: 10.1310/6GL4-UM7X-519H-9JYD

Fey, N. P., Klute, G. K., and Neptune, R. R. (2011). The influence of energy storage and return foot stiffness on walking mechanics and muscle activity in below-knee amputees. *Clin. Biomech.* 26, 1025–1032. doi: 10.1016/j.clinbiomech.2011.06.007

Fitzpatrick, N., Smith, T. J., Pendegrass, C. J., Yeadon, R., Ring, M., Goodship, A. E., et al. (2011). Intraosseous transcutaneous amputation prosthesis (ITAP) for limb salvage in 4 dogs. *Vet. Surg.* 40, 909–925. doi: 10.1111/j.1532-950X.2011.00891.x

Florez, J. M., Shah, M., Moraud, E. M., Wurth, S., Baud, L., Von Zitzewitz, J., et al. (2017). Rehabilitative soft exoskeleton for rodents. *IEEE Trans. Neural Syst. Rehabil. Eng.* 25, 107–118. doi: 10.1109/TNSRE.2016.2535352

Forssberg, H. (1979). Stumbling corrective reaction: a phase-dependent compensatory reaction during locomotion. *J. Neurophysiol.* 42, 936–953. doi: 10.1152/jn.1979.42.4.936

Garcia, E., Arevalo, J. C., Munoz, G., and Gonzalez-De-Santos, P. (2011). On the biomimetic design of agile-robot legs. *Sensors* 11, 11305–11334. doi: 10.3390/s111211305

Goslow, G. E. Jr., Reinking, R. M., and Stuart, D. G. (1973). The cat step cycle: hind limb joint angles and muscle lengths during unrestrained locomotion. *J. Morphol.* 141, 1–41. doi: 10.1002/jmor.1051410102

Graczyk, E. L., Schiefer, M. A., Saal, H. P., Delhaye, B. P., Bensmaia, S. J., and Tyler, D. J. (2016). The neural basis of perceived intensity in natural and artificial touch. *Sci. Transl. Med.* 8:362ra142. doi: 10.1126/scitranslmed.aaf5187

Gregor, R. J., Maas, H., Bulgakova, M. A., Oliver, A., English, A. W., and Prilutsky, B. I. (2018). Time course of functional recovery during the first 3 mo after surgical transection and repair of nerves to the feline soleus and lateral gastrocnemius muscles. *J. Neurophysiol.* 119, 1166–1185. doi: 10.1152/jn.00661.2017

Gregor, R. J., Smith, D. W., and Prilutsky, B. I. (2006). Mechanics of slope walking in the cat: quantification of muscle load, length change, and ankle extensor EMG patterns. *J. Neurophysiol.* 95, 1397–1409. doi: 10.1152/jn.01300.2004

Hagberg, K., and Branemark, R. (2009). One hundred patients treated with osseointegrated transfemoral amputation prostheses–rehabilitation perspective. *J. Rehabil. Res. Dev.* 46, 331–344. doi: 10.1682/JRRD.2008.06.0080

Herr, H. M., and Grabowski, A. M. (2012). Bionic ankle-foot prosthesis normalizes walking gait for persons with leg amputation. *Proc. Biol. Sci.* 279, 457–464. doi: 10.1098/rspb.2011.1194

Hof, A. L., Van Bockel, R. M., Schoppen, T., and Postema, K. (2007). Control of lateral balance in walking. Experimental findings in normal subjects and above-knee amputees. *Gait Posture* 25, 250–258. doi: 10.1016/j.gaitpost.2006.04.013

Hoy, M. G., and Zernicke, R. F. (1985). Modulation of limb dynamics in the swing phase of locomotion. *J. Biomech.* 18, 49–60. doi: 10.1016/0021-9290(85)90044-2

Jaegers, S. M., Arendzen, J. H., and De Jongh, H. J. (1995). Prosthetic gait of unilateral transfemoral amputees: a kinematic study. *Arch. Phys. Med. Rehabil.* 76, 736–743. doi: 10.1016/S0003-9993(95)80528-1

Jarrell, J., Farrell, B. J., Kistenberg, R. S., Dalton, J. F. T., Pitkin, M., and Prilutsky, B. I. (2018). Kinetics of individual limbs during level and slope walking with a unilateral transtibial bone-anchored prosthesis in the cat. *J. Biomech.* doi: 10.1016/j.jbiomech.2018.05.021 [Epub ahead of print].

Juhnke, D. L., Beck, J. P., Jeyapalina, S., and Aschoff, H. H. (2015). Fifteen years of experience with Integral-Leg-Prosthesis: cohort study of artificial limb attachment system. *J. Rehabil. Res. Dev.* 52, 407–420. doi: 10.1682/JRRD.2014.11.0280

Kannape, O. A., and Herr, H. M. (2014). Volitional control of ankle plantar flexion in a powered transtibial prosthesis during stair-ambulation. *Conf. Proc. IEEE Eng. Med. Biol. Soc.* 2014, 1662–1665. doi: 10.1109/EMBC.2014.6943925

Kannape, O. A., and Herr, H. M. (2016). Split-belt adaptation and gait symmetry in transtibial amputees walking with a hybrid EMG controlled ankle-foot prosthesis. *Conf. Proc. IEEE Eng. Med. Biol. Soc.* 2016, 5469–5472. doi: 10.1109/EMBC.2016.7591964

Klishko, A. N., Farrell, B. J., Beloozerova, I. N., Latash, M. L., and Prilutsky, B. I. (2014). Stabilization of cat paw trajectory during locomotion. *J. Neurophysiol.* 112, 1376–1391. doi: 10.1152/jn.00663.2013

Leijendekkers, R. A., Staal, J. B., Van Hinte, G., Frolke, J. P., Van De Meent, H., Atsma, F., et al. (2016). Long-term outcomes following lower extremity press-fit bone-anchored prosthesis surgery: a 5-year longitudinal study protocol. *BMC Musculoskelet. Disord.* 17:484. doi: 10.1186/s12891-016-1341-z

Li, G., Schultz, A. E., and Kuiken, T. A. (2010). Quantifying pattern recognition-based myoelectric control of multifunctional transradial prostheses. *IEEE Trans. Neural Syst. Rehabil. Eng.* 18, 185–192. doi: 10.1109/TNSRE.2009.2039619

Markin, S. N., Lemay, M. A., Prilutsky, B. I., and Rybak, I. A. (2012). Motoneuronal and muscle synergies involved in cat hindlimb control during fictive and real locomotion: a comparison study. *J. Neurophysiol.* 107, 2057–2071. doi: 10.1152/jn.00865.2011

McFadyen, B. J., Lavoie, S., and Drew, T. (1999). Kinetic and energetic patterns for hindlimb obstacle avoidance during cat locomotion. *Exp. Brain Res.* 125, 502–510. doi: 10.1007/s002210050708

Mich, P. M. (2014). The emerging role of veterinary orthotics and prosthetics (V-OP) in small animal rehabilitation and pain management. *Top. Companion Anim. Med.* 29, 10–19. doi: 10.1053/j.tcam.2014.04.002

Ollivier-Lanvin, K., Krupka, A. J., Auyong, N., Miller, K., Prilutsky, B. I., and Lemay, M. A. (2011). Electrical stimulation of the sural cutaneous afferent nerve controls the amplitude and onset of the swing phase of locomotion in the spinal cat. *J. Neurophysiol.* 105, 2297–2308. doi: 10.1152/jn.00385.2010

Ortiz-Catalan, M., Hakansson, B., and Branemark, R. (2014). An osseointegrated human-machine gateway for long-term sensory feedback and motor control of artificial limbs. *Sci. Transl. Med.* 6:257re256. doi: 10.1126/scitranslmed.3008933

Park, H., Mehta, R., Deweerth, S. P., and Prilutsky, B. I. (2015). "Modulation of afferent feedback from paw pad afferents affects interlimb coordination and adaptation to split-belt treadmill locomotion in the cat," in *Society for Neuroscience Meeting*, Chicago, IL.

Park, H., Oh, K., Prilutsky, B. I., and Deweerth, S. P. (2016). "A real-time closed-loop control system for modulating gait characteristics via electrical stimulation of peripheral nerves," in *Proceedings of the 2016 IEEE Biomedical Circuits and Systems Conference (BioCAS)*, (Shanghai: IEEE), 95–98. doi: 10.1109/BioCAS.2016.7833733

Pitkin, M., Cassidy, C., Muppavarapu, R., and Edell, D. (2012). Recording of electric signal passing through a pylon in direct skeletal attachment of leg prostheses with neuromuscular control. *IEEE Trans. Biomed. Eng.* 59, 1349–1353. doi: 10.1109/TBME.2012.2187784

Pitkin, M., Raykhtsaum, G., Pilling, J., Shukeylo, Y., Moxson, V., Duz, V., et al. (2009). Mathematical modeling and mechanical and histopathological testing of porous prosthetic pylon for direct skeletal attachment. *J. Rehabil. Res. Dev.* 46, 315–330. doi: 10.1682/JRRD.2008.09.0123

Prilutsky, B. I., Herzog, W., and Leonard, T. (1996). Transfer of mechanical energy between ankle and knee joints by gastrocnemius and plantaris muscles during cat locomotion. *J. Biomech.* 29, 391–403. doi: 10.1016/0021-9290(95)00054-2

Prilutsky, B. I., Maas, H., Bulgakova, M., Hodson-Tole, E. F., and Gregor, R. J. (2011). Short-term motor compensations to denervation of feline soleus and lateral gastrocnemius result in preservation of ankle mechanical output during locomotion. *Cells Tissues Organs* 193, 310–324. doi: 10.1159/000323678

Prilutsky, B. I., Sirota, M. G., Gregor, R. J., and Beloozerova, I. N. (2005). Quantification of motor cortex activity and full-body biomechanics during unconstrained locomotion. *J. Neurophysiol.* 94, 2959–2969. doi: 10.1152/jn.00704.2004

Quevedo, J., Stecina, K., Gosgnach, S., and Mccrea, D. A. (2005). Stumbling corrective reaction during fictive locomotion in the cat. *J. Neurophysiol.* 94, 2045–2052. doi: 10.1152/jn.00175.2005

Rabago, C. A., Aldridge Whitehead, J., and Wilken, J. M. (2016). Evaluation of a powered ankle-foot prosthesis during slope ascent gait. *PLoS One* 11:e0166815. doi: 10.1371/journal.pone.0166815

Realmuto, J., Klute, G., and Devasia, S. (2011). Nonlinear passive cam-based springs for powered ankle prostheses. *J. Med. Dev.* 9:011007. doi: 10.1115/1.4028653

Roche, E. T., Wohlfarth, R., Overvelde, J. T., Vasilyev, N. V., Pigula, F. A., Mooney, D. J., et al. (2014). A bioinspired soft actuated material. *Adv. Mater.* 26, 1200–1206. doi: 10.1002/adma.201304018

Sawicki, G. S., and Ferris, D. P. (2009). A pneumatically powered knee-ankle-foot orthosis (KAFO) with myoelectric activation and inhibition. *J. Neuroeng. Rehabil.* 6:23. doi: 10.1186/1743-0003-6-23

Shultz, A. H., Lawson, B. E., and Goldfarb, M. (2016). Variable cadence walking and ground adaptive standing with a powered ankle prosthesis. *IEEE Trans. Neural Syst. Rehabil. Eng.* 24, 495–505. doi: 10.1109/TNSRE.2015.2428196

Struyf, P. A., Van Heugten, C. M., Hitters, M. W., and Smeets, R. J. (2009). The prevalence of osteoarthritis of the intact hip and knee among traumatic leg amputees. *Arch. Phys. Med. Rehabil.* 90, 440–446. doi: 10.1016/j.apmr.2008.08.220

Takahashi, K. Z., Lewek, M. D., and Sawicki, G. S. (2015). A neuromechanics-based powered ankle exoskeleton to assist walking post-stroke: a feasibility study. *J. Neuroeng. Rehabil.* 12:23. doi: 10.1186/s12984-015-0015-7

Tan, D. W., Schiefer, M. A., Keith, M. W., Anderson, J. R., Tyler, J., and Tyler, D. J. (2014). A neural interface provides long-term stable natural touch perception. *Sci. Transl. Med.* 6:257ra138. doi: 10.1126/scitranslmed.3008669

Tkach, D. C., Young, A. J., Smith, L. H., Rouse, E. J., and Hargrove, L. J. (2014). Real-time and offline performance of pattern recognition myoelectric control using a generic electrode grid with targeted muscle reinnervation patients. *IEEE Trans. Neural Syst. Rehabil. Eng.* 22, 727–734. doi: 10.1109/TNSRE.2014.2302799

Wand, P., Prochazka, A., and Sontag, K. H. (1980). Neuromuscular responses to gait perturbations in freely moving cats. *Exp. Brain Res.* 38, 109–114. doi: 10.1007/BF00237937

Weber, H. F. (1965). Pulse-width modulation DC motor control. *IEEE Trans. Ind. Electron. Control Instrum.* 1, 24–28. doi: 10.1109/TIECI.1965.229545

Conflict of Interest Statement: The authors declare that the research was conducted in the absence of any commercial or financial relationships that could be construed as a potential conflict of interest.